International Journal of Coal Geology 228 (2020) 103554

Contents lists available at ScienceDirect

International Journal of Coal Geology

journal homepage: www.elsevier.com/locate/coal

Thermal and depositional history of Early-Permian Rio Bonito Formation of southern Paraná Basin – Brazil

Marcos Müller Bicca[a,*], Wolfgang Kalkreuth[a], Taís Freitas da Silva[a], Christie Helouise Engelmann de Oliveira[b], Frederico Antonio Genezini[c]

[a] Instituto de Geociências, Universidade Federal do Rio Grande do Sul, Porto Alegre, Brazil
[b] Universidade do Vale do Rio dos Sinos, São Leopoldo, Rio Grande do Sul, Brazil
[c] Instituto de Pesquisas Energéticas e Nucleares da Universidade de São Paulo, São Paulo, Brazil

ARTICLE INFO

Keywords:
Paraná Basin
Vitrinite reflectance
Apatite Thermochronology
Burial history

ABSTRACT

The Paraná Basin is a large volcano-sedimentary basin with a complex depositional history from Ordovician to the Cretaceous period. During Permian significant amounts of organic-rich beds accumulated within the Rio Bonito and Irati formations representing deposition in coastal (deltaic and barrier lagoon) and shallow marine environments, respectively. In this work, the thermal history of these beds is examined from 16 vitrinite reflectance analyses of coal beds (Rio Bonito Formation), integrated with previous data on coal rank, and 21 apatite fission-track (AFT) analyses, collected from 17 well profiles in the south of the Paraná Basin. Coal samples showed three different maturity levels. Two with reflectances of 0.4–0.6 and 0.6–0.8%Rr formed by the natural burial history of the basin (the latter is restricted to the Torres Syncline area). In contrast, the third group reached much higher values (1.0–5.0%Rr) related to intrusive igneous rocks. The AFT data show thermal consistency with the reflectance values. The sandstone samples related to the two lower reflectance patterns were partially reset, preserving AFT ages older than the stratigraphic age of the bed. Otherwise, the samples severely affected by the magmatism have Cretaceous and Early Cenozoic ages, but some were much younger than the last magmatic event, implying deep burial before cooling onset. The mean track length distribution of the partially reset samples is short due to the inheritance of tracks preserved from basement cooling history. However, the population of fully reset samples gives crucial information on the maximum temperature reached and the age when cooling started. At these conditions, around 1.0 to 3.0 km of the Paraná Basin sequences would have been removed from the surface of the studied areas by erosion since Cretaceous. Regional variations in the amounts of removed sections were controlled by the structural framework, mostly regional NW-SE and NE-SW oriented structures.

1. Introduction

Coal deposits occur in the southern part of the Paraná Basin, Brazil, in an intracratonic volcano-sedimentary sequence distributed in southern Brazil, Paraguay, Argentina, and northwest Uruguay (Fig. 1A). This basin has a large and complex depositional history that began in the Ordovician to the Cretaceous period, culminating with extensive volcanism produced during the Gondwana break-up (Milani and de Wit, 2008). The coalfields occur in the Early-Permian Rio Bonito Formation, mostly in the Rio Grande do Sul and Santa Catarina states (Kalkreuth et al., 2006) and minor in Paraná and São Paulo states (Fig. 1B and C). The Rio Bonito Formation comprises fluvial/deltaic to shallow marine sequences deposited between 298 and 285 Ma (U–Pb ages from tonsteins and tuff horizons after Guerra-Sommer et al., 2008a, 2008b, 2008c; Mori et al., 2012; Simas et al., 2012; Cagliari et al., 2014; Cagliari et al., 2016; Griffis et al., 2018).

Coal seams start to generate gas after reaching high volatile bituminous rank (%Rr ≥0.7%Rr) (Choate et al., 1986). Studies developed along-strike of the basin margin at the Rio Grande do Sul and Santa Catarina in southern Brazil found significant accumulations of natural gas adsorbed in coal seams collected between 450 and 650 m depth (Kalkreuth et al., 2006, 2010, 2013a).

In view of this, the objective of this work was to investigate the characteristics of the Paraná Basin in terms of lateral and vertical variations in coals maturity levels, and the influence of post-deposition tectonic and exhumation events by the analysis of 16 new vitrinite

* Corresponding author.
E-mail address: marcos.bicca@ufrgs.br (M.M. Bicca).

https://doi.org/10.1016/j.coal.2020.103554
Received 31 January 2020; Received in revised form 10 June 2020; Accepted 21 June 2020
Available online 15 July 2020

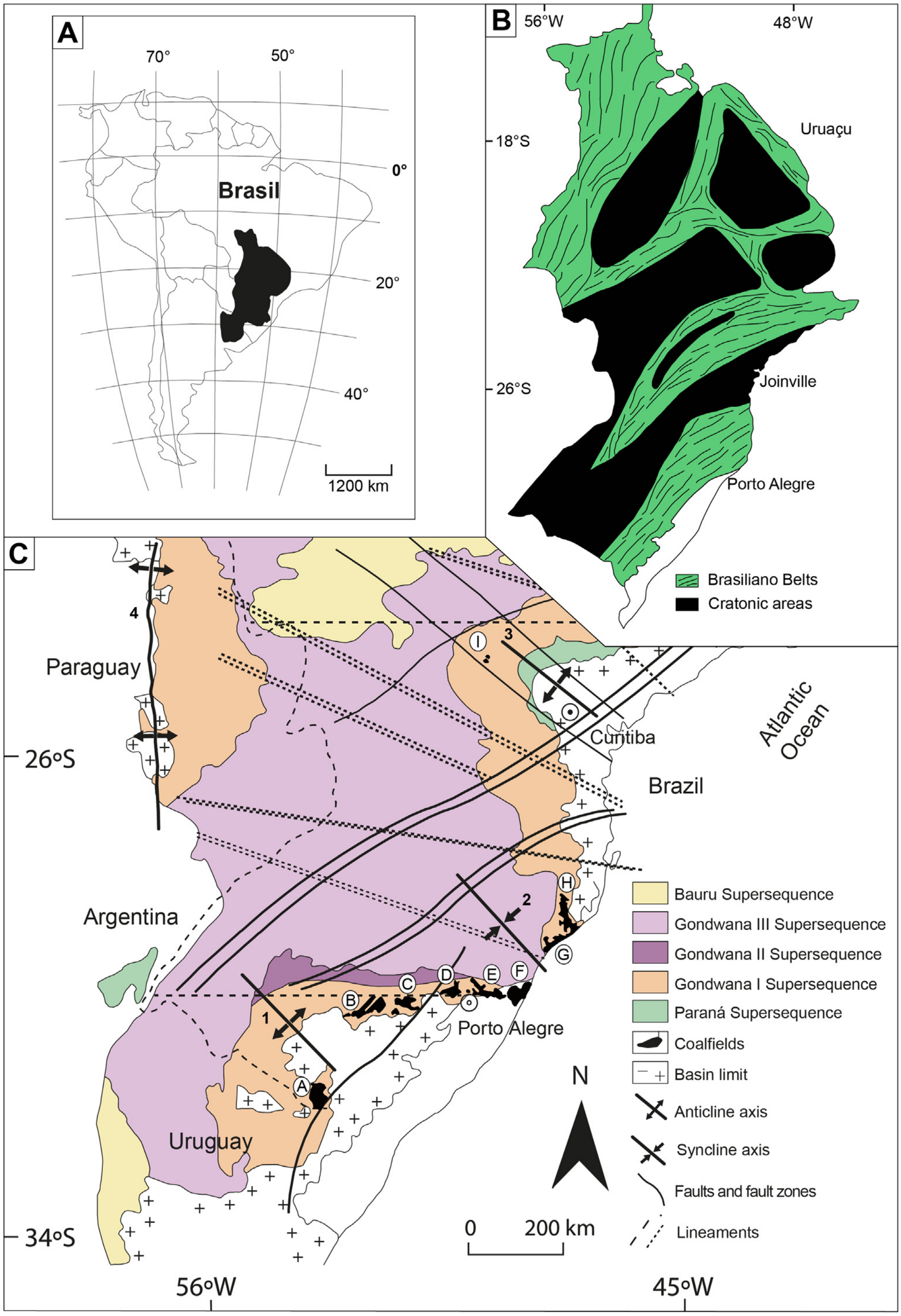

Fig. 1. A) Paraná Basin location in South America plate; B) Simplified geotectonic basement of the Paraná Basin in Brazil; C) Simplified geologic and structural map of southern Paraná Basin (Holz et al., 2006) with main coalfields (Kalkreuth et al., 2013a). 1) Rio Grande Arc; 2) Torres Syncline; 3) Ponta Grossa Arc; 4) Asunción Arc. Coalfields: A) Candiota; B) Leão-Butiá; C) Charqueadas-Santa Rita; D) Faxinal; E) Morungava-Chico Lomã; F) Santa Terezinha; G) Southern Santa Catarina; H) Criciúma e Lauro Müller; I) Paraná.

reflectance data for coalfields of southern Paraná Basin. Additionally, the apatite fission-track (AFT) technique was applied to sandy layers of Rio Bonito, Palermo and Rio do Rastro formations with a total of 21 samples at coastal and inland areas to reconstruct the burial history of each analyzed site and evaluate the thermal variations in coal seams and sedimentary rocks.

2. Geological setting

The Paraná Basin lies on igneous and metamorphic belts of Proterozoic to Paleozoic in age (Fig. 1B). These geotectonic domains constitute a dense structural framework, which contributes dramatically to subsidence, magmatism, and hydrothermal events during basin development (Milani and de Wit, 2008). The depositional cycles of the Paraná Basin were controlled by sea-level variations and distal tectonic events on the south and southwestern margin of Gondwana, generating regional scale sequence limits (Zerfass et al., 2004; Holz et al., 2006; Milani and de Wit, 2008).

The sedimentary infill of the Paraná Basin comprises six supersequences bounded by regional unconformities (Fig. 1): Rio Ivaí (Ordovician–Silurian), Paraná (Devonian), Gondwana I (Carboniferous–Early Triassic), Gondwana II (Middle-Late Triassic), Gondwana III and Bauru (Early Cretaceous). The Rio Ivaí and Paraná, represent the two basal supersequences comprising two transgressive-regressive marine cycles, but the Rio Ivaí Supersequence (base of the basin) occurs only northwards and is not discussed in this paper. The depositional base of the Gondwana I Supersequence is marked by a ~ 50 Ma erosive gap and has the highest potential for hydrocarbon generation restricted to the Rio Bonito and Irati formations. The deposition of Gondwana II, Gondwana III, and Bauru supersequences culminating with the eruption of extensive magmatism (Paraná-Etendeka Province) related to the opening of the Atlantic Ocean (Milani and de Wit, 2008) and age of 134 Ma to 119 Ma (Hartmann et al., 2019).

2.1. Stratigraphy of Gondwana I Supersequence

The base of the Gondwana I Supersequence is characterized by glacial-related continental and marine deposits of the Itararé Group, deposited directly on the Paleoproterozoic basement rocks. The group comprises diamictites, sandstones, rhythmites, shales, and conglomerates with a maximum depositional age of 307.7 ± 3.1 Ma (U–Pb analysis by LA-MC-ICPMS) determined from volcanic ash zircons found in this group (Cagliari et al., 2016). The top of the Itararé Group marks a sequence boundary, which separates Itararé Group glacial-marine sediments from the Rio Bonito Formation (Holz et al., 2002).

The Rio Bonito Formation comprises subarcosean conglomerates, sandstones, and siltstones, with a cross and planar stratifications, covered by laterally discontinuous mudstones and thin coal seams of fluvial origin at the base of the formation, and coal seams formed in a lagoonal back-barrier setting having a thickness of up to 3 m (Kalkreuth et al., 2010). Above this package, coal seams laterally associate with quartz-sandstones and shales, with lenticular or wavy laminations. The sandstones present planar and through-cross stratifications, with levels of flaser, wavy, and (abundant) hummocky laminations, characterizing an estuarine depositional environment evolving into a lagoon-barrier system (Holz et al., 2002), where marshes formed in back-barrier lagoon bodies. River deposits consist of coarse sandstone facies with current structures. This change in the depositional environment marks the beginning of a transgressive cycle (Kalkreuth et al., 2010). The depositional age of Rio Bonito Formation was determined by U–Pb (CA-TIMS) as 298.23 ± 0.31 Ma (Griffis et al., 2018).

The Palermo Formation overlays the Rio Bonito Formation strata, with a sequence formed by fine sediments with hummocky and wavy stratification and deposited in a shallow marine environment (Fig. 2; Holz et al., 2010). This system comprises the maximum flooding of a regional transgression with a maximum depositional age of around 280 Ma (Canile et al., 2016). A fall of the base level marks the transition to the Irati Formation that corresponds to a marine transgression. This formation extends over most of the Paraná Basin and is subdivided into Taquaral Member (base) and the Assistência Member (top) (Fig. 2). The Taquaral Member is composed of siltstones and dark shales, corresponding to shallow marine deposits with restricted connections with the open sea. In contrast, the Assistência Member has shales and organic-rich shales interbedded with limestones indicating deposition in deep-sea conditions (Holz et al., 2010). Geochronological dating of bentonite beds defines a depositional age of 278.4 ± 2.2 Ma (Santos et al., 2006) and 282 Ma (Canile et al., 2016) for the Irati Formation.

A new fall in the base level marks the transition between the Irati and Serra Alta formations, mainly represented by the absence of bituminous shales and thin breccia beds, conglomerates, and intraformational sandstones. Laminated black and light grey shales dominate in the Serra Alta Formation, in addition to carbonate concretions and thin layers of sandstones, suggesting a wave-dominate marine environment of low oxygen concentration (Holz et al., 2002).

The transition to the Teresina Formation is gradual (Fig. 2). Thus, as in the Serra Alta Formation, strata of Teresina also have a marine origin evidenced by coastal floodplain and sediments of the coastal plain, with little carbonate precipitation. This formation is mostly represented by interlaminated shales with very fine sandstones, presenting linsen and flaser laminations, and hummocky cross-stratifications (Holz et al., 2010).

Finally, the Rio do Rastro Formation is a normal grading succession subdivided in the Serrinha Member (Fig. 2), formed by shales and fine sandstones in shallow lakes occasionally influenced by storms and river incursions, which transition to medium to thick sandstones of the Morro Pelado Member (Fig. 2). The Morro Pelado Member depositional environment is generally attributed to meandering, lacustrine, deltaic, eolic and alluvial fluvial environments. At the top of the Rio do Rastro Formation occurs a significant erosive discordance that separates the Gondwana I and Gondwana II Supersequences (Holz et al., 2010). The youngest zircons dated in this formation show ages from 266 Ma to 252 Ma (Canile et al., 2016) assumed in this work as the main depositional interval of the Rio do Rastro Formation.

3. Previous coal rank studies in the southern Paraná Basin

3.1. Summary of coal rank determinations

The coalfields of Rio Grande do Sul show a northeasterly increasing trend in coals rank. The lowest rank occurs in Candiota (subbituminous) while the highest is in the Santa Terezinha coalfield (high-volatile A bituminous; Fig. 3). In Candiota and Leão-Butiá coalfields, vitrinite reflectances are in the range of 0.4% to 0.6%Rr (Kalkreuth et al., 2006, 2013a, 2013b). The variation in %Rr observed at Candiota, Leão and Butiá, over the depth interval of around 42 m, is related to facies changes and depositional environment (Holz and Kalkreuth, 2004), mostly those seams related to beds of marine origin (Kalkreuth et al., 2006).

In the Santa Terezinha coalfield (Fig. 1C), there is an increase in coals rank towards the north of the coalfield. Here the coal seams occur between 400 and 1000 m depths (Kalkreuth et al., 2006). The heat-affected coals in contact with igneous intrusion are in semianthracite and anthracite rank levels (2.0–5.0%Rr). Westwards, in the Morungava-Chico-Lomã coalfields, the coals rank decrease (0.5–0.7%Rr), when not in contact with intrusive rocks, and the coal seams occur at shallower depths. Vitrinite reflectance values of Santa Catarina coal seams range from 0.60 to 1.63% Rr, which correspond to rank levels of high volatile bituminous C to medium volatile bituminous (Kalkreuth et al., 2010; Costa et al., 2014).

In the Paraná State, at Figueira and Sapopema regions (Figs. 1C and 3), studies of coal rank have been rare. The main study of coal rank is that of Levandowski and Kalkreuth (2009), presenting petrographic and chemical characterization of the coal used at the Figueira Power Plant (Fig. 1C). Reported vitrinite reflectance values between 0.61 and 0.73% Rr suggests rank levels varying from high volatile B and C bituminous coal.

3.1.1. Influence of magmatism on coal maturity

The vitrinite reflectance analyses in the southern Paraná Basin show distinct maturation levels varying laterally and with burial depth. Higher reflectance values were measured near the contact of coals with intrusive rocks, where reflectances are higher than 1.0%Rr, increasing the potential for gas generation (Kalkreuth et al., 2006; Lourenzi and Kalkreuth, 2014; Simão and Kalkreuth, 2017). The coalification profiles of the Santa Terezinha and Morungava coalfields (Fig. 4) show a characteristic pattern where reflectances increase exponentially close to the igneous rock contact where coal can reach maturity levels of

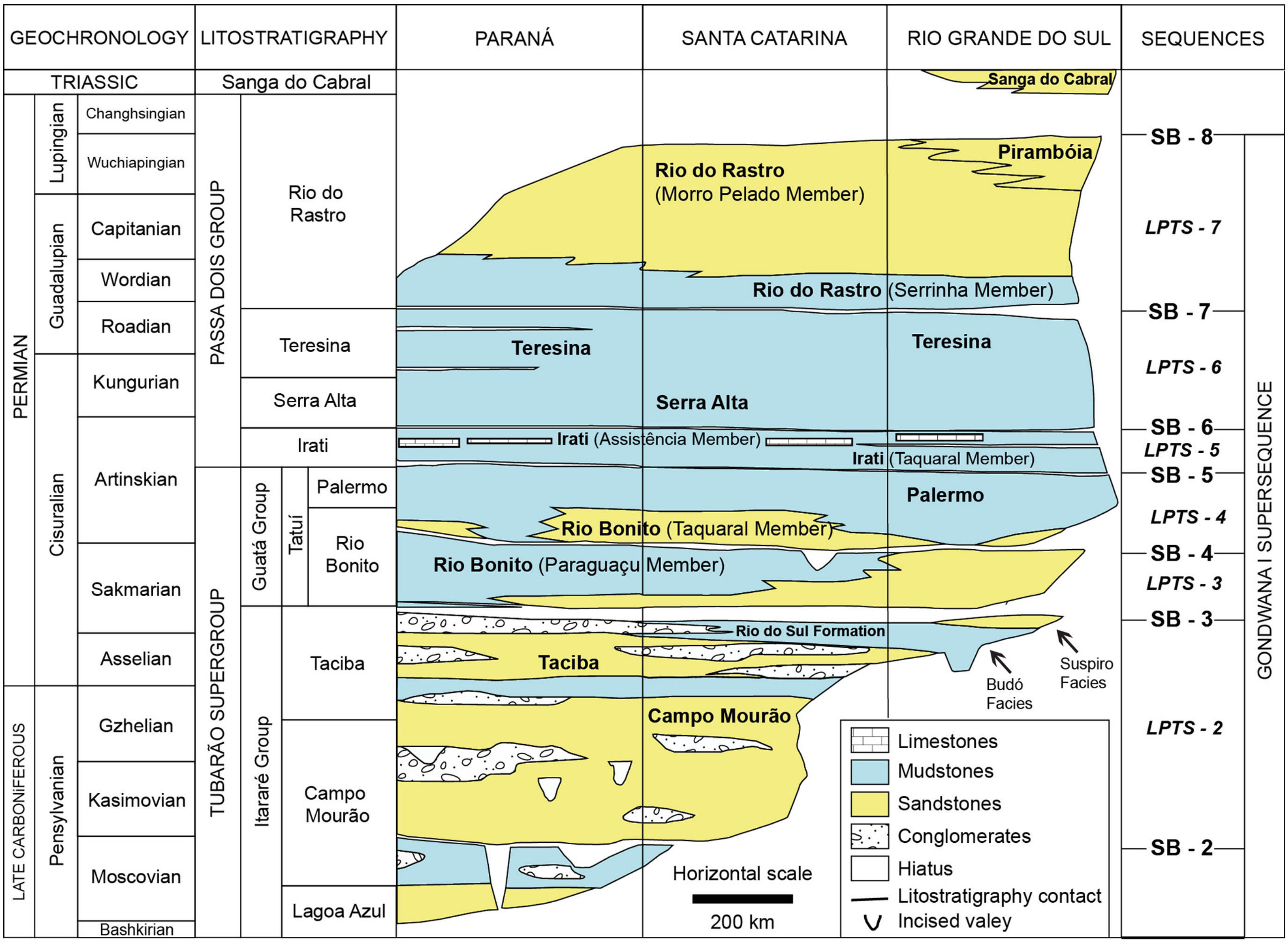

Fig. 2. A schematic stratigraphic model identifying the main formations that makes up the Gondwana I Supersequence in the Rio Grande do Sul, Santa Catarina and Paraná states (modified from Holz et al., 2010).

anthracite and form natural coke (Fig. 4; Kalkreuth et al., 2013a; Simão and Kalkreuth, 2017).

The central aspect refers to the amplitude reached by the thermal flow induced by magmatism, which is best observed in the coalification profile of the Morungava well. In general, the maximum distance of thermal influence in the southern Paraná Basin is proportional to the intrusion thickness (Fig. 4). The thermal halo of an intrusion with a thickness of 20 m will correspond to a distance of 20 m above and below from the contact, decreasing exponentially until the normal maturation levels found in the Paraná Basin (Fig. 4; Araújo et al., 2000). The thermal halo thickness may vary slightly depending on the temperature of the intrusive rock, being the upper halo slightly thicker than the lower (Goodarzi et al., 2019). Additionally, the improvement in gas diffusion of coals near intrusive igneous rocks increases by a factor of two (Saghafi et al., 2008).

3.2. Thermochronology

There are only a few studies of thermochronology applied to the Paraná Basin rocks. Gallagher et al. (1994, 1995) applied AFT technique in 68 Precambrian basement rocks and sedimentary (Paraná Basin) samples from onshore rift margin in southeast Brazil, and 18 of these samples located in adjacent areas of this work (Fig. 5). The sedimentary samples from the Paraná Basin have AFT ages younger than their stratigraphic ages (Carboniferous to Cretaceous), and confined mean track length measurements (MTL) range from 12 to 13.5 μm, indicating some post-depositional annealing. According to (Gallagher et al., 1994, 1995), the spread in the individual crystal ages suggests they have not undergone total annealing since deposition. Besides, the relatively short MTL and broad length distributions indicate that these samples do not record the magmatic event but represent partially reset or mixed AFT ages. Central age dispersion is > 10%, but can be higher than 60% due to differences in the pre-depositional fission-track characteristics of the apatites (e.g., inherited or provenance ages) or natural variations in apatite composition (Green et al., 1989).

Two basalt samples of the Serra Geral Formation were also analyzed, showing long MTL (14–15 μm) and AFT ages close to magmatism age of ca. 130 Ma age (Gallagher et al., 1994, 1995). The single-grain ages have low dispersion suggesting that they have not been significantly annealed since magmatism. However, samples from the basalt-sediment contact of the Jurassic Botucatu Formation have younger and spread AFT ages (65–120 Ma) and lower MTL than the basalt, which requires additional annealing in the younger samples. According to the authors, the data suggest that the coastal plain experienced ca. 3 km of erosion and the hinterland little more than 1 km (Gallagher et al., 1994).

4. Material and methods

4.1. Sampling strategy

The present study samples were collected from 17 wells distributed

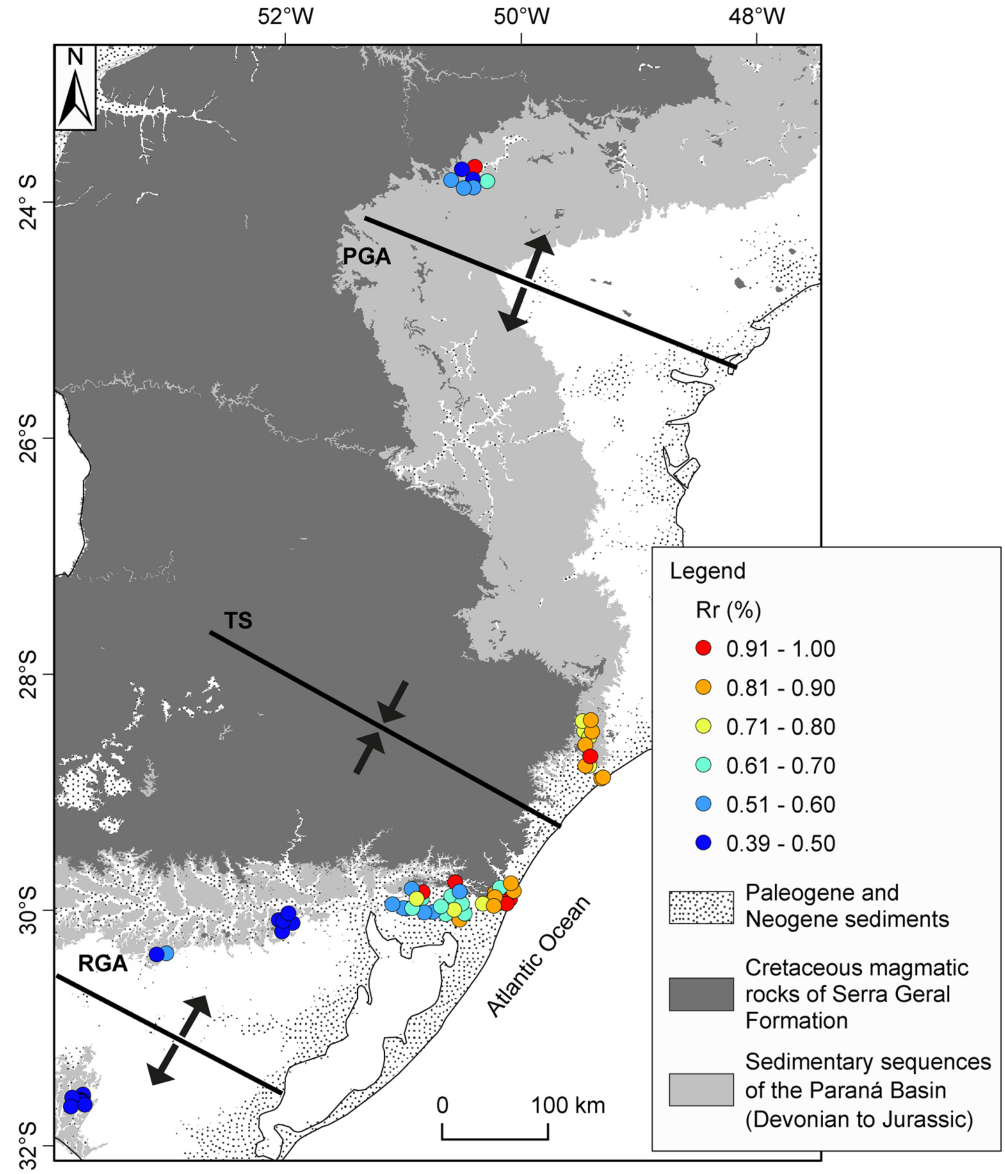

Fig. 3. Geological map of the study area (after Perrotta et al., 2004; Lopes et al., 2004; Wildner et al., 2008) with vitrinite reflectance values of this and previous works (Kalkreuth et al., 2006, 2010, 2013a; Silva et al., 2008; Levandowski and Kalkreuth, 2009; Lourenzi and Kalkreuth, 2014; Costa et al., 2014). When more than one reflectance measurement is available per well the average value was shown. RGA – Rio Grande Arc; TS – Torres Syncline; PGA – Ponta Grossa Arc.

on the southern edge of the Paraná Basin (Figs. 6, 7 and 8). Samples of coal seams from the Rio Bonito Formation were collected for vitrinite reflectance analysis and the sedimentary rocks adjacent to them for AFT analysis. Since the wells belong to exploratory private mining companies, sometimes there was no coal left in the boxes to be sampled; thus, only the sedimentary rocks were taken.

The sampling was controlled by factors such as the depth of the coal seams, the presence of igneous intrusions in the profile and its thickness, and the sandstone maturity. The latter was considered for AFT analyses since apatite grains do not survive long-distance transport. Sandstones samples were collected from all 17 well profiles. However, some samples did not have enough or suitable apatite grains for analysis and were not showed in the profiles. In addition, the position of the wells sampled in relation to the main regional structures was also considered. Special attention was given to samples collected in the Torres Synclinal structure, considering the greater thickness of the preserved sequences, suggesting more significant subsidence during the deposition of the Paraná Basin sequences.

4.2. Vitrinite reflectance analyses

Sample preparation and analytical procedure for vitrinite reflectance analyses were performed according to Bustin et al. (1989) and conducted at the Universidade Federal do Rio Grande do Sul, Brazil. The coal samples preparation consisted of crushing the samples in a jaw crusher and homogenize them applying a mesh sieve of < 4.5 mm. Particles with a size fraction between 0.25 and 0.80 mm were embedded in epoxy resin for the construction of polished blocks used in the vitrinite reflectance analyses. The random reflectance measurements (%Rr) were carried out on vitrinite particles in reflected white light with removed polarizer and magnification of 500× (ISO-7404/5, 2009). The measurements were taken in 100 points on each sample using A LEICA DM6000 M microscope and a Discus-Fossil software. The microscope was calibrated before each analysis using precision yttrium-aluminum-garnet standard with a reflectance value of 0.895%Rr under oil immersion and an optical black (zero) glass.

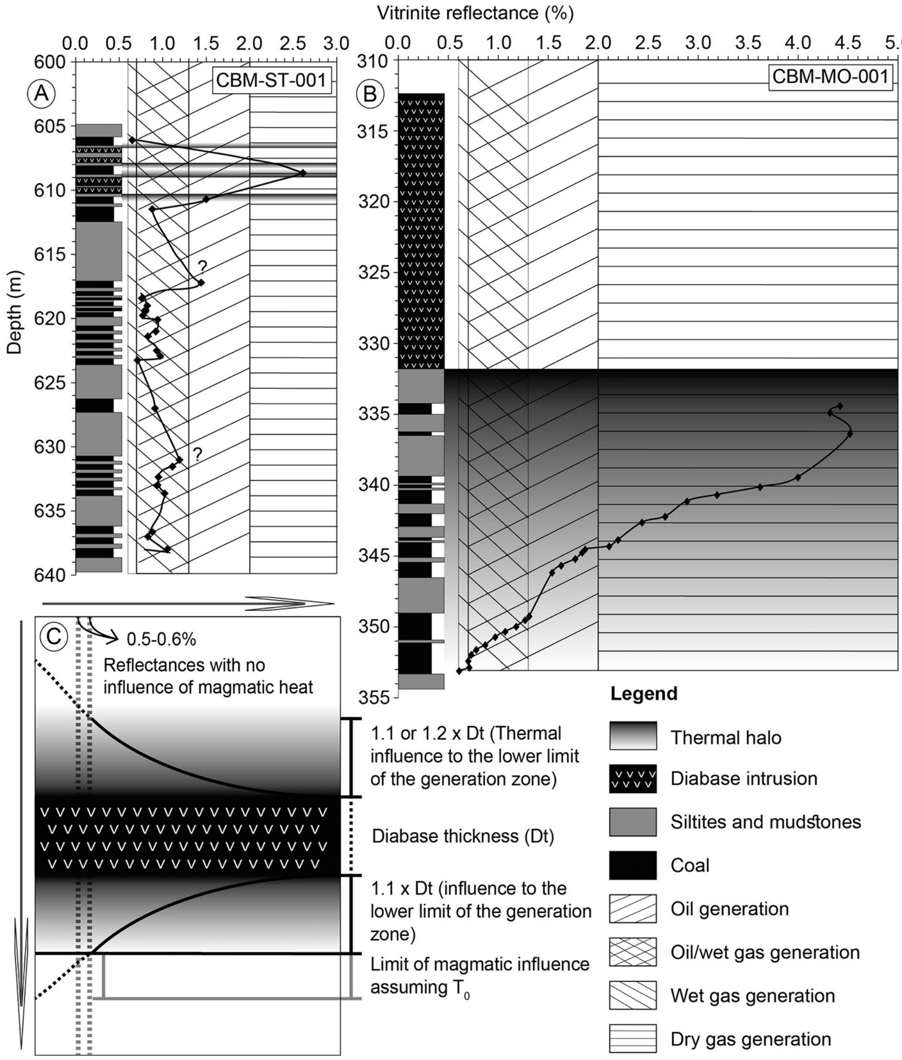

Fig. 4. Coalification profiles at Santa Terezinha (A) and Morungava (B) of Rio Grande do Sul (Kalkreuth et al., 2006; Simão and Kalkreuth, 2017) with a sketch showing the thermal halo dimensions based in the vitrinite reflectance data of coals of Rio Grande do Sul (C).

4.3. Burial history and Time-Temperature Index calculations

The depositional and tectonic history of the southern Paraná Basin sequences was derived as a time-depth curve, drawn over a temperature plot that reflects the present and past gradient of the area (Kalkreuth and McMechan, 1984). The method adopted here is better described in Kalkreuth and McMechan (1984) and Kalkreuth et al. (1989). To the coalification estimates of Rio Bonito Formation coals the Lopatin (1971), and Waples (1980) method was used. The method is based on the premise that temperature is the main factor affecting coalification (Kalkreuth and McMechan, 1984), and the reaction rates double for each 10 °C increase in temperature (Lopatin, 1971). The thickness of the sedimentary pile between each 10 °C interval depends on the geothermal gradient applied.

The individual TTI values of each 10 °C of increment in a determined time span was calculated with the equation: TTI = $_{i=tp}\Sigma_{i=0}$ TTI(i) + $2^{-10.5+(temp(i)x0.1)(\Delta t)}$, where i = tp is the present time; temp(i) is the mean temperature of a time interval (Δt); $i = O$ is the period of deposition. The sum of all individual TTI values is than applied to the equation: TTI = $n_{max}\Sigma n_{min}(\Delta t_n)(r^n)$, where n_{max} and n_{min}, where the n-values is the highest and lowest temperature intervals of the model, based in the geological data (the 100–110 °C interval is assigned a value of $n = 1$), Δt_n is the amount of time present in a given temperature interval (at each 10 °C increment), and r is an empirically rate factor equal to 2 (Waples, 1980). The solution of this equation allows to calculate the maximum vitrinite reflectance value (R_{max}%), from the formula of Waples (1980): log R_{max} = −0.4769 + 0.2801(log TTI) -0.007472 (log TTI)^2. The maximum reflectance represents the rank level of a given sample since the beginning of the deposition. Since random reflectance values of vitrinite were used in this research, it was necessary to convert it to maximum reflectance using the equation (Ting, 1978): Rmax% = 1.066 x Rr%.

The present-day geothermal gradient of 27.5 °C/km (Hamza et al., 2005) was used as a constant through time. The reconstruction of the incomplete profiles was based on the correlation with nearby wells with a complete record. The Serra Geral Formation thicknesses range from 400 and 800 m at the basin margin, however, it can reach 1500–1800 m in the depocenter (Gallagher et al., 1994), suggesting that up to 1000 m of basalts have been removed from the basin top sequences. The post-depositional history (erosion) was estimated from the thermal modeling of AFT data.

4.4. Apatite fission track

The apatite fission-track (AFT) method is an excellent tool for studying the thermal history of sedimentary basins in a temperature range of 60 °C and 110 ± 10 °C (Laslett et al., 1987; Green et al., 1986). The thermal interval of AFT unstable zone is referred to as

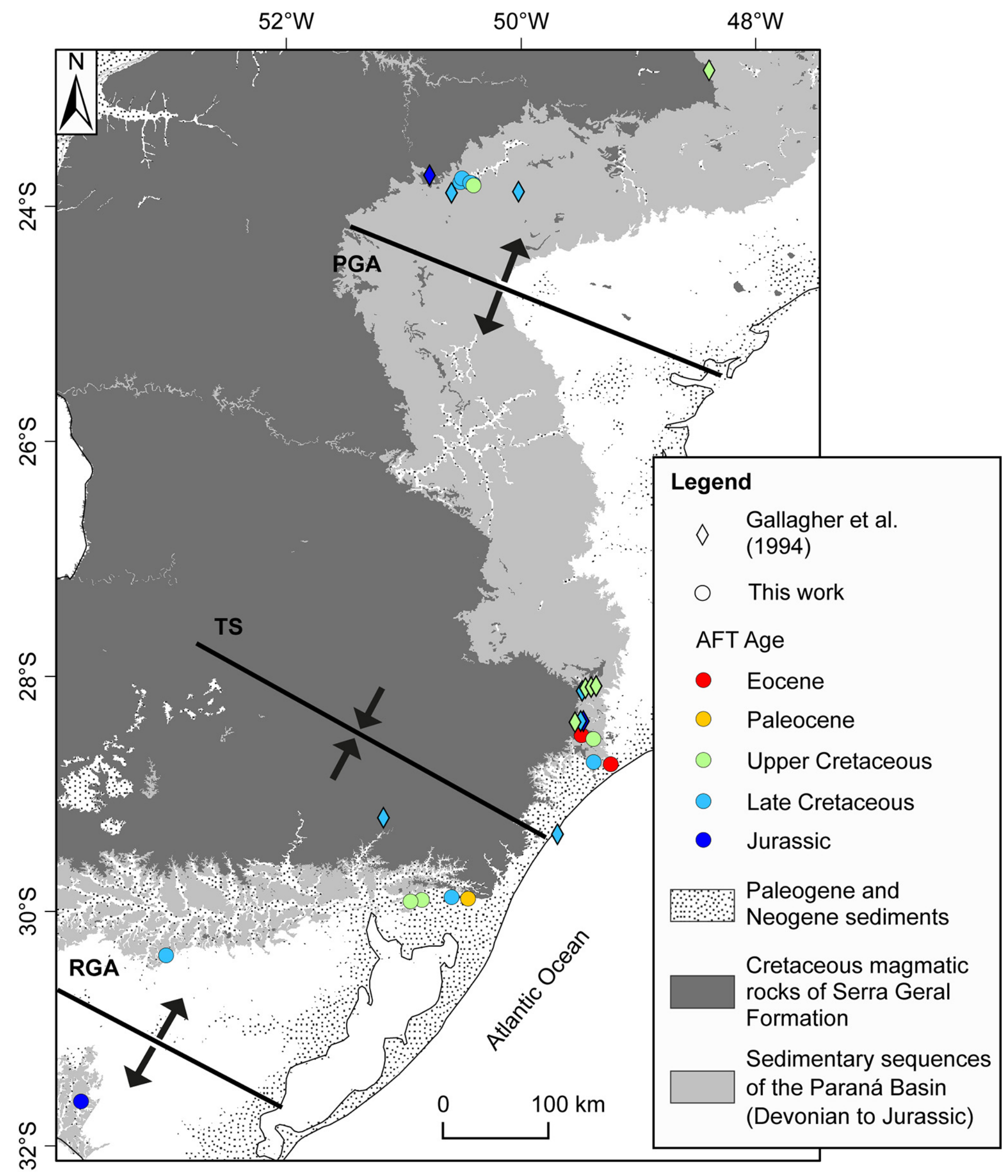

Fig. 5. Simplified geological map of the study area (after Perrotta et al., 2004; Lopes et al., 2004; Wildner et al., 2008) with central ages of this work and the sedimentary-volcanic samples of Gallagher et al. (1994).

partial annealing zone (PAZ). The analyzes of AFT length distribution allows establishing the thermal behavior of a given sample during periods of burial and erosion in a sedimentary basin (Green et al., 2004) or events of hydrothermal alteration and magmatism (Gallagher et al., 1998). A complete description of the method can be found in Wagner and Van den Haute (1992), Gallagher et al. (1998), Gleadow et al. (2002).

4.4.1. Analytical procedures for AFT determinations

The samples were prepared using conventional methods as crushing, sieving, magnetic, heavy liquid, and hand-picking techniques and mounted in epoxy resin, performed at Universidade Federal do Rio Grande do Sul (UFRGS). The spontaneous FTs were revealed by etching the samples with 5.5 M HNO_3 at 21 °C for 20 s (Ketcham et al., 2007). The External Detector Method (Gleadow, 1981) was used for AFT dating. Neutron irradiation was performed in the IEA-R1 Nuclear Reactor of the IPEN (Nuclear and Energetic Research Institute), São Paulo, Brazil. After irradiation, the induced FTs were revealed by etching the detectors with 48% HF for 18 min.

The zeta calibration method (Hurford, 1990) was used for AFT age calculations with a CN_2 dosimeter glass and the Durango apatite age standard. Each grain and confined track founded were counted and measured in each sample. The orientation of the confined tracks relative to the c-axis was also measured, and the inverse modeling was performed with projected mean track length (MTL). Ages are given as pooled or central ages with their respective percent variation (Galbraith and Laslett, 1993). The $\chi 2$ test was used to determine the presence of one or more age populations (Galbraith and Laslett, 1993). The online version of the software "IsoplotR" was used for this purpose (Vermeesch, 2018). D_{par} measurements (etch pit diameter) was the proxy used for apatite kinetics (Donelick et al., 2005), and an average value was determined for each grain.

4.4.2. Thermal history modeling based on AFT analyses

Thermal history modeling is based on the complex relationship between the AFT age, MTL and kinetic parameters to derive independent time-temperature histories for individual samples (Gallagher, 2012). The HeFTy 1.9.3 program (Ketcham, 2005) was used here for apatite thermal history modeling using the multikinetic annealing model of Ketcham et al. (2007) and the D_{par} values as kinetic

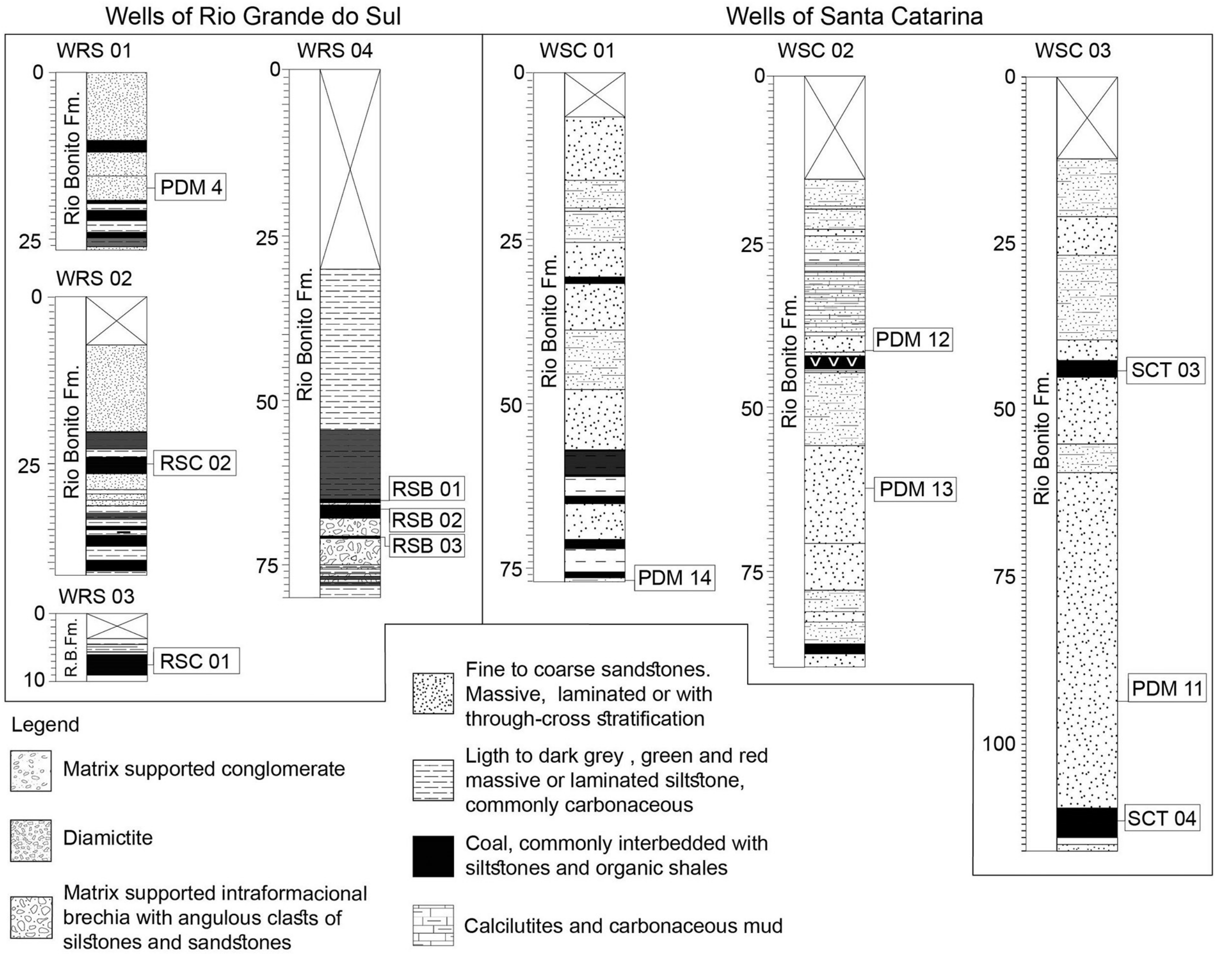

Fig. 6. Well logs of Capané (WRS 01, 02 and 03), Butiá (WRS 04), and southern Santa Catarina. Well logs with sample position.

parameters. Each time-temperature (t–T) history model was run with 10,000 interactions for each sample to generate statistically acceptable models (Ketcham, 2005). When coal and sandstone samples were in contact or close to each other in the profile, the vitrinite reflectance was added to modeling.

Due to the complex and long-term depositional history of the Paraná Basin, seven constraints were used for the thermal modeling of samples. They mostly represent periods of sedimentation and magmatism in the basin. The AFT data set distribution and patterns were also considered for constrains definition. Every constrain adopted for AFT modeling in this paper is described below:

a) Depositional age – the time interval of deposition used derive from geochronological (U–Pb dating) data, mostly from ash-flow tuffs recognized in several Permian beds of the Paraná Basin. When isotopic data is not available, the palynological record was used as a general reference for deposition time.
b) Precambrian basement – the only one sample of a granitic rock comes from the bottom of Morungava well, where the Rio Bonito sequences are deposited directly over the granite, meaning it was at the surface at the time of deposition. In this case, a constrain of 310 ± 10 Ma (temperature of 20 ± 10 °C) was used for this sample modeling.
c) End of deposition of Gondwana I Supersequences (250 ± 10 Ma and 40 ± 10 °C) – a period of no deposition and/or basin erosion, except for samples of Butiá region, where during Triassic Period a local rift basin was developed and was filled with thick sedimentary sequences. The temperature was estimated from the thickness measured in each well log and assuming the present-day geothermal gradient.
d) Botucatu Formation (140 ± 10 Ma and 40 ± 10 °C) – this formation precedes the final phase of deposition within the basin.
e) Serra Geral Formation (134 ± 5 Ma) – At this period, samples show two distinct patterns. Some samples have been fully reset, implying thermal (magmatic) heating (100 ± 10 °C), and others have reached temperatures around or lower than 100 °C reflecting heating by burial only (90 ± 10 °C).
f) Present surface temperature – the present-day temperatures of each sample were estimated from the 27.5 °C/km gradient (present) plus the measured depth of samples summed with the average annual surface temperature (20 °C).

5. Results

5.1. Coal rank (vitrinite reflectance) analyses

Coals of Butiá and Capané (RS) areas are subbituminous, determined by reflectances varying between 0.41 and 0.56%Rr (Table 1), in agreement with other reflectance values determined in nearby areas (Kalkreuth et al., 2006; Silva et al., 2008). In these areas, there are not many occurrences of intrusions between the basin layers, so the reflectances are commonly low around the Rio Grande Arc (Fig. 3), where coals are close to the surface (< 100 m).

The southern Santa Catarina samples have high reflectance values of 2.11% and 1.49%Rr (SCT 01 and SCT 02), but one sample of well WSC 03 gives a value of 0.84%Rr (Table 1; SCT 03). The higher reflectances

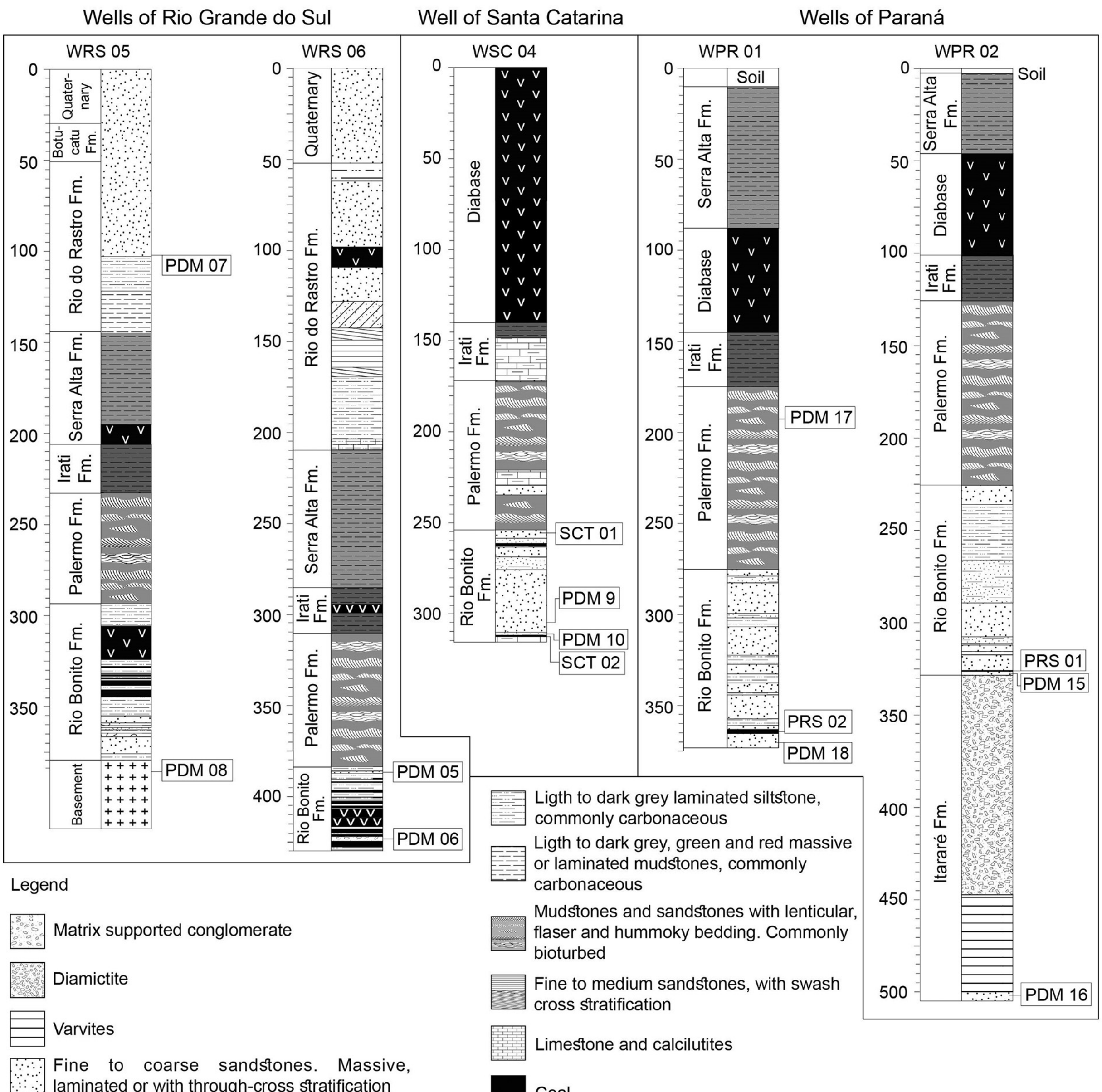

Fig. 7. Logs of well with the most complete register of basin sequences. Rio Grande do Sul - Morungava (WRS 05) and Chico-Lomã (WRS 06) of Simão and Kalkreuth (2017) and Levandowski (2013), respectively; Southern Santa Catarina (WSC 04); Paraná (WPR 01 and 02). The sample position is indicated in each profile.

result, most likely, from maturation influenced by nearby intrusions. Still, the lowest one agrees with the reflectances measured in samples of wells located at the coast and reflectance values of most coal seams in the Criciuma mining area (Kalkreuth et al., 2010), and may approximate the temperatures related to the depositional history of the basin. Vitrinite reflectances of well WSC 04 (Fig. 6) decrease from 2.11% to 1.49%Rr with depth. This inverted trend is related to a thick (134 m) intrusion placed at the top of the sequence. Nevertheless, part of the volcanic rock must have been removed by erosion, because the present thickness would not be enough to affect the bottom-most sample (Table 1), assuming the range of thermal influence of igneous intrusions described earlier. Coal samples SCT 03 and 04 (Fig. 6 and Table 1), show the expected increasing reflectance trend with depth, from 0.84% to 1.07%Rr at the base, although, thermal variation is too high considering the small distance (70 m) between samples, requiring additional heat, possibly from a near dike or sill.

The coal seams analyzed from the coalfield region in Paraná show low rank levels (0.4 to 0.6%Rr on average), except for a value of 0.96% Rr (Table 1). These measurements are consistent with those of Levandowski and Kalkreuth (2009) with averages of 0.6 and 0.7%Rr at the Figueira mine. The absence of igneous intrusions in the profile of well WPR 04 (Fig. 8) suggests a lateral heat contribution from an intrusion close to this well. The local alteration suggests a possibly hosted in NE-SW structures, which are very common in the area (Araújo et al., 2005).

The reflectances from the southern Paraná Basin appear to have been influenced by factors other than subsidence and associated paleotemperatures, commonly taken as the main influence on coal rank. Apparently, the facies changes and depositional environment have influenced the reflectance level of vitrinite, mostly those overlain by marine strata showing very low reflectance values (Holz and Kalkreuth, 2004).

5.2. Apatite thermochronology

AFT results for 21 samples of sedimentary rocks belonging to the

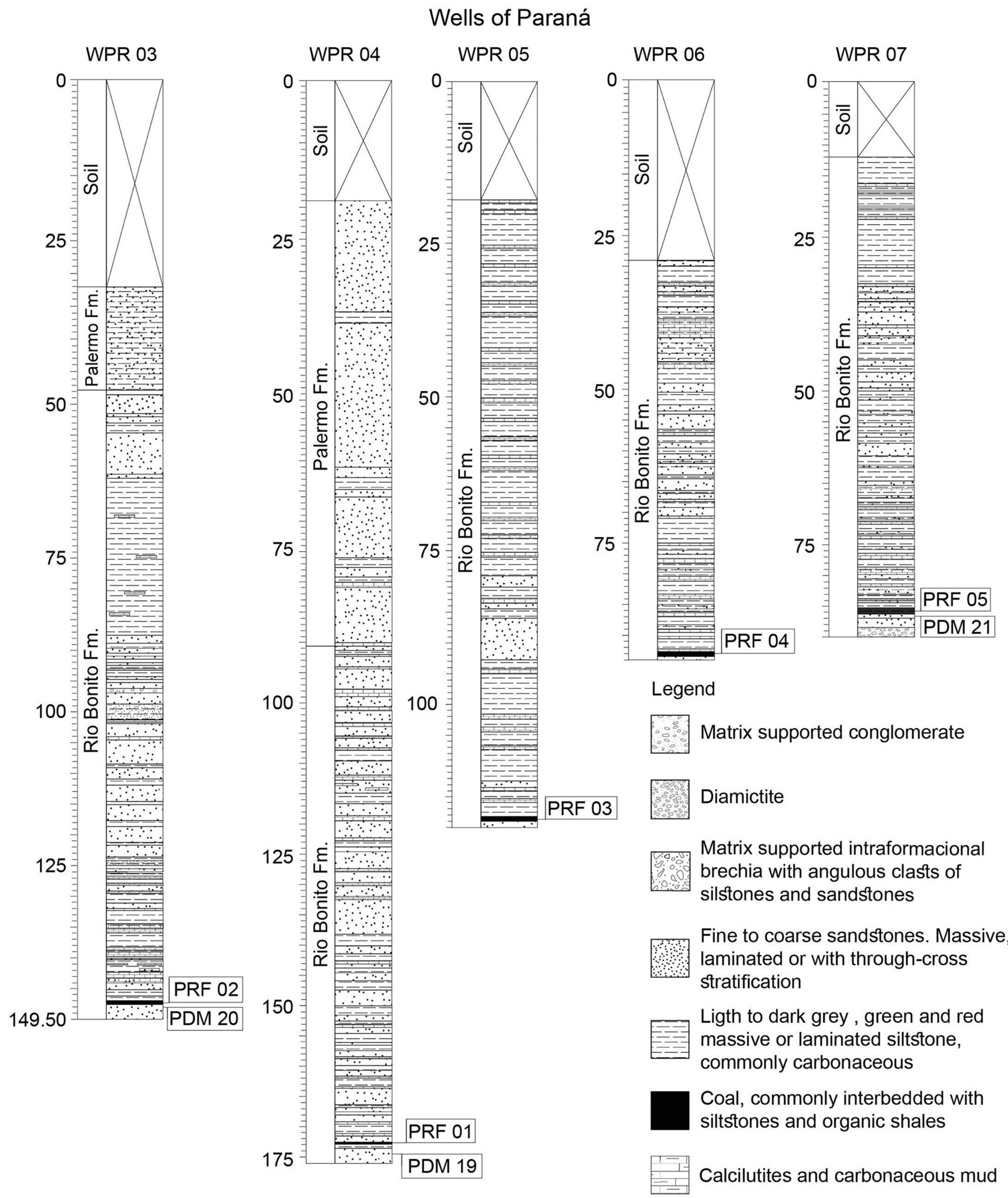

Fig. 8. Well logs of Figueira region of northern Paraná State, with sample locations.

Rio Bonito, Palermo, and Rio do Rastro formations are presented in Table 2, and AFT age distribution is shown in Figs. 9, 10, and 11. Most samples have only a few analyzable apatite grains but revealed significant information concerning the thermal basin history. The data show two different thermal patterns (Table 2 and Figs. 9, 10, and 11), which are consistent with the rank levels of interbedded coals.

The first group of samples comprises FTs that were not fully reset after basin deposition and magmatism (Fig. 11). These samples are from Candiota, Capané, and Butiá (RS), and at Figueira and Sapopema (PR) areas, where reflectance values are lower than 0.6%Rr. There are two age populations, with χ^2 tests lower than 0.5% (Table 2). One population is older than the final magmatism within the basin, with ages from Carboniferous (Upper Pennsylvanian) to Lower Cretaceous, and other much younger (Paleogene; Table 2; Figs. 9, 10 and 11). Consequently, the measured MTL are short (between 8 and 10 µm) due to the inheritance of tracks already shortened in the source rock mixed with tracks shortened by burial in the basin. Otherwise, these data were compatible with the corresponding reflectances in the sampled wells, determining valuable information regarding deposition patterns of the area.

Differently, fission tracks of the second group have been fully reset, most with two age populations and MTL between 10 and 12 µm (Fig. 9). AFT ages are Paleocene and Miocene, being much younger than basin magmatism, suggesting high burial depth before cooling onset during Cenozoic. These samples are from the Torres Syncline area, except those near igneous intrusions (Fig. 9). The kinetic parameters of the samples are all similar, with D_{par} values between 4 and 7 µm (Table 2).

The partial annealing of some samples may not be related to

Table 1
Vitrinite reflectance data of coal samples.

Sample	Lat	Long	Depth (m)	Rr%
RIO GRANDE DO SUL (RS)				
Butiá				
RSB 01	−30.108	−51.937	64.20–64.35	0.42
RSB 02			65.85–85.90	0.43
RSB 03			70.00–70.05	0.41
Capané				
RSC 01	−30.374	−53.051	9	0.45
RSC 02	−30.367	−53.026	24.30–24.38	0.56
SOUTHERN SANTA CATARINA (SC)				
Treviso				
SCT 01	−28.535	−49.421	261.00	2.11
SCT 02			310.00	1.49
SCT 03	−28.480	−49.463	43.00	0.84
SCT 04			110.00	1.07
NORTHERN PARANÁ (PR)				
Sapopema				
PRS 01	−23.791	−50.515	336.00–336.50	0.54
PRS 02	−23.759	−50.502	368–368.80	0.44
Figueira				
PRF 01	−23.798	−50.434	174.00–174.10	0.96
PRF 02	−23.805	−50.411	147.00–147.10	0.49
PRF 03	−23.819	−50.412	117.95–118.05	0.52
PRF 04	−23.815	−50.403	92.50–92.60	0.51
PRF 05	−23.820	−50.406	84.45–84.60	0.61

compositional variations of the apatite grains of the samples (such as F and Cl contents), but rather to the thermal flux variability in the sandstones. This variation is caused by the presence of water in high porosity rocks and cementation between grains of a sandstone directly influences the intensity with which the thermal flow acts over the rock. Water-saturated samples have commonly higher conductivity than anhydrous rocks (Guo et al., 2017). Considering that most of the analyzed samples belong to the Rio Bonito Formation, deposited in coastal and shallow marine environments with high variability of carbonate cementation, vertical variations in temperature intensity is expected within the sandy layers. Also, some samples collected in this work represent ranges up to 60 cm thick (Table 2).

6. Apatite fission-track thermal modeling

Based on FTs parameters and geological background of the area, inversion models for the samples were developed using pre-defined constraints (Figs. 12, 13). The sample PDM 4 at Capané coalfield (Fig. 12A) presented the thermal history with the lowest maximum temperature (ca. 76 °C), reached at 133 Ma, being consistent with the low coal maturity of this region (< 0.6%Rr). Rock cooling was slow (4 °C) to 70 Ma, briefly accelerating until 22 Ma, reaching temperatures around 64 °C, when a constant cooling brought the sample to present-day conditions (Fig. 12B).

Samples PDM 5-6 (Fig. 12A, C and D) and PDM 7–8 (Fig. 12A, E and F) have mostly the same thermal history, with maximum temperatures around 100 °C at 133 Ma, except for sample PDM 5, that registered the highest heating to 138 °C, at the same time. This last sample started cooling vigorously at 100 Ma to surface conditions reached around 50 Ma when a smooth reheating started (Fig. 12C). The other three samples started cooling after reaching the maximum temperature, but very slowly, to 80–95 °C until 98 Ma. Cooling to 70–80 °C occurs at 60 Ma, from where samples cool to surface conditions, after what they were heated up to approximately 5 °C.

All samples of the southern Santa Catarina coalfield (Fig. 12A) show a similar thermal history during basin sedimentation until 134 Ma when a severe heat-affected PDM 9–10 and PDM 11 samples (Fig. 13A and B). These wells are at the northern edge of Torres Syncline, and both reach around 130 °C, after deposition and magmatism at 133 Ma, which is in agreement with the high vitrinite reflectance values measured in coal samples of each well (Table 2). The model suggests that temperature decrease abruptly to 100–110 °C at 115 Ma, interpreted as the end of magmatic influence because the four samples of southern Santa Catarina show almost the same thermal history after 115 Ma (Fig. 13). Sample PDM 12–13 (Fig. 13C) show a slower cooling history, residing for about 70 Ma at temperatures near 100 °C. Only at 40 Ma sample temperature reduce 10 °C and cooling to surface conditions started (Fig. 13C). Nevertheless, sample PDM 14 (Fig. 13D) reached the lowest temperatures (90 °C) in comparison to the other wells, and constantly cools to around 65 °C at 40 Ma, after what cooled to surface conditions (Fig. 13D).

The inverse modeling of samples from wells of northern Paraná (Fig. 14) have similar thermal characteristics and are compatible with maturity levels defined by vitrinite reflectance measurements. The two samples PDM 15 and PDM 16 (Fig. 14A and B) have identical thermal histories preceding maximum temperature, but slightly different cooling histories, possibly due to the absence of confined track measurements of PDM 15 sample (Fig. 14C). This sample records continuous cooling after reaching 88 °C at 133 Ma, while sample PDM 16 shows episodic cooling at 100 Ma (82 °C), 40 Ma (78 °C) and 10 Ma (60 °C). Assuming the distance between samples (176 m) and the thermal variation between them (6 °C), it is possible to estimate an approximate paleogradient of 34 °C/km during the final deposition phase of the basin, when the maximum temperatures were reached.

Samples PDM 17-18 (Fig. 14C and D) have similar thermal histories to samples PDM 15-16. The sample PDM 17, taken within the interval of diabase thermal influence (Fig. 7), and for this reason, it has a maximum temperature of 105 °C at 134 Ma, dropping sharply to 123 Ma to 82 °C (Fig. 14C). From this moment on, the thermal histories of the two samples record identical patterns, constantly cooling down to 70 °C at 40 Ma. An accelerated final cooling event brought the samples to the current temperature. Assuming that the temperature of 82 °C, recorded after the end of the magmatic influence on sample PDM 17, represents the basin temperature, the two samples in this well define a paleogradient of approximately 32 °C/km, close to that determined for samples PDM 15 and PDM 16.

The sample PDM 19 reached the highest maximum temperature (123 °C), among samples from this area, at 131 Ma (Fig. 14E), comparable to the 0.9%Rr reflectance measured. After that, the model shows an abrupt reduction in temperature to 103 °C at 110 Ma, from where it continuously cooled to present thermal conditions. Nevertheless, sample PDM 20 recorded a similar cooling history, but reached a maximum of 98 °C at 132 Ma, from where it rapidly cooled (20 Ma) to 80 °C (Fig. 14F). After that sample took 80 Ma to cool until 60 °C, achieving present-day conditions in the last 20 Ma (Fig. 14F).

7. Temperature and maturity levels variations

The coalification profiles influenced by the intrusion, presented earlier in Fig. 3, and the regional trend of coalification from south to north, define two populations of reflectances probably generated by burial: i) 0.4 to 0.6%Rr - at the hinterland of Rio Grande do Sul (Candiota, Capané, Butiá) and northern Paraná; and ii) 0.6 to 0.8%Rr - in the Torres Synclinal region (at the margin) in the south of Santa Catarina, Santa Terezinha, Chico-Lomã and Morungava. The temperatures determined by AFT thermal models support this data because the maturation kinetics of vitrinite is similar to the annealing kinetics of AFT (Duddy et al., 1998). According to the models, the maximum temperatures in the first group of reflectances range between 70 and 90 °C, whereas the second comprises temperatures of 90 to 110 °C. Around the thermal halo developed by intrusions, AFT data recorded temperatures up to 135 °C, due to the limit of the technic, but reflectances up to 5.0% Rr, like those seen in Morungava and Chico Lomã coalification profile, require much higher temperatures. The definition of these temperature ranges was crucial for burial history reconstructions since they allow

Table 2
Apatite fission track data from wells of Southern Paraná Basin.

Sample	Lat	Long	Depth	N	ρs (Ns)	ρi (Ni)	ρd (Nd)	P (χ2)	U Content	Age* ± 1σ	Dpar	n	Mean track length	Mean track length	Std. Dev.
	S	E	(m)		(x10^5)	(x10^5)	(x10^5)	(%)	(ppm)	(Ma)	(μm)		(μm) ± 1σ	(μm) ± 1σ (projected)	(μm)
RIO GRANDE DO SUL															
Candiota															
PDM 1	−31.616	−53.747	71.07–71.62	6	22.6 (64)	11.0 (31)	21.4 (4099)	7.7	1.9	232 ± 15.25					
PDM 2			51.84–51.94	5	11.1 (25)	89.2 (20)	20.0 (5849)	28.0	1.6	149.6 ± 12.23					
PDM 3			45.40–46.18												
Butiá															
PDM 4	−30.373	−53.024	16.80–17.20	15	52.7 (163)	38.2 (118)	16.9 (4955)	0.0	8.2	207 ± 14	3.96				
Chico-Lomã															
PDM 5	−29.878	−50.590	384.36–384.59	17	11.2 (819)	13.9 (937)	20.2 (4397)	0.0	25.2	143.1 ± 11.96	4.25	5	11.62 ± 0.3	12.00 ± 0.45	0.66
PDM 6			431.29–431.45	27	52.3 (327)	81.6 (510)	20.5 (4323)	0.0	14.5	59.1 ± 8.2	4.10	2	9.73 ± 0.03	10.94 ± 0.08	1.16
Morungava															
PDM 7	−29.901	−50.842	106.10–106.40	17	10.9 (605)	97.7 (541)	19.2 (5626)	0.0	18.5	130.1 ± 11.40	5.08	20	9.89 ± 0.43	10.74 ± 0.52	1.92
PDM 8			386.58–386.94	24	49.0 (460)	54.1 (507)	18.9 (5414)	4.0	20.5	90.9 ± 12	4.25	10	9.72 ± 0.49	10.76 ± 0.5	1.54
SOUTHERN SANTA CATARINA															
Treviso															
PDM 9	−28.535	−49.421	305.05–305.59	2	42.6 (27)	18.9 (12)	18.1 (5291)	8.8	3.8	221.6 ± 14.89					
PDM 10			309.12–309.22	5	55.9 (109)	10.9 (213)	19.9 (4472)		20.1	77.0 ± 8.78	6.68				
PDM 11	−28.480	−49.463	95.10–95.38	6	48.4 (134)	10.0 (277)	19.9 (4472)	0.7	18.4	57.3 ± 7.57	6.59	3	10.62 ± 0.44	11.40 ± 0.70	0.76
Içara															
PDM 12	−28.750	−49.237	40.80–41.44	3	32.6 (40)	78.1 (96)	18.3 (4844)	0.0	15.6	46.2 ± 6.79	4.03	3	8.41 ± 0.19	10.26 ± 0.84	0.34
PDM 13			61.80–62.22	24	30.3 (289)	80.0 (764)	18.5 (5402)	0.0	15.8	52.7 ± 7.26	4.44	8	8.95 ± 0.51		1.44
PDM 14	−28.730	−49.361	68.40–68.84	33	8.61 (124)	13.5 (195)	9.30 (9302)	0.0	18.2	168.6 ± 12.98	3.89	16	8.67 ± 0.37		1.49
SOUTHERN PARANÁ															
Sapopema															
PDM 15	−23.791	−50.515	327.90–328.30	5	42.7 (45)	29.4 (31)	18.1 (5291)	4.4	5.9	221.1 ± 14.87					
PDM 16			503.20–503.70	45	82.7 (1399)	72.5 (1226)	17.7 (5179)	0.0	14.9	140.6 ± 12.25	4.17	29	8.72 ± 0.33	9.72 ± 0.33	1.78
PDM 17	−23.759	−50.502	179.90–180.50	36	64.1 (534)	61.7 (514)	18.6 (4771)	0.0	12.1	130 ± 11.40	4.65	6	9.59 ± 0.34	10.43 ± 0.34	0.84
PDM 18			366.80–367.20	41	12.2 (854)	11.7 (819)	16.6 (4844)	0.0	25.7	149.9 ± 12.24	3.94	24	8.90 ± 0.28	9.96 ± 0.28	1.38
Figueira															
PDM 19	−23.798	−50.434	174.10–174.75	10	48.0 (109)	51.5 (117)	20.8 (4248)	0.4	9.0	138.9 ± 11.78	4.66				
PDM 20	−23.805	−50.411	148.75–149.30	71	71.1 (1782)	50.3 (1259)	17.7 (5179)	0.0	10.4	167.7 ± 12.83	3.67	23	9.01 ± 0.54	10.05 ± 0.54	1.22
PDM 21	−23.820	−50.406	85.20–85.80	8	75.4 (205)	76.8 (209)	16.9 (4955)	8.7	16.6	139.4 ± 11.81					

N: number of grains analyzed to determine track densities; ρ_s: measured spontaneous track density; N_S: number of spontaneous tracks counted; ρ_i: measured induced track density; Ni: number of induced tracks counted; ρd: track density measured in external detector adjacent to glass dosimeter during irradiation; Nd: number of tracks counted in determining ρd; P (χ2): the probability of obtaining observed χ2 value for n degrees of freedom (n = number of crystals −1); n: number of confined tracks lengths measured. * Apatite ages calculated using a zeta of 105.9 for CN2 glass. Analyst: CHEO.

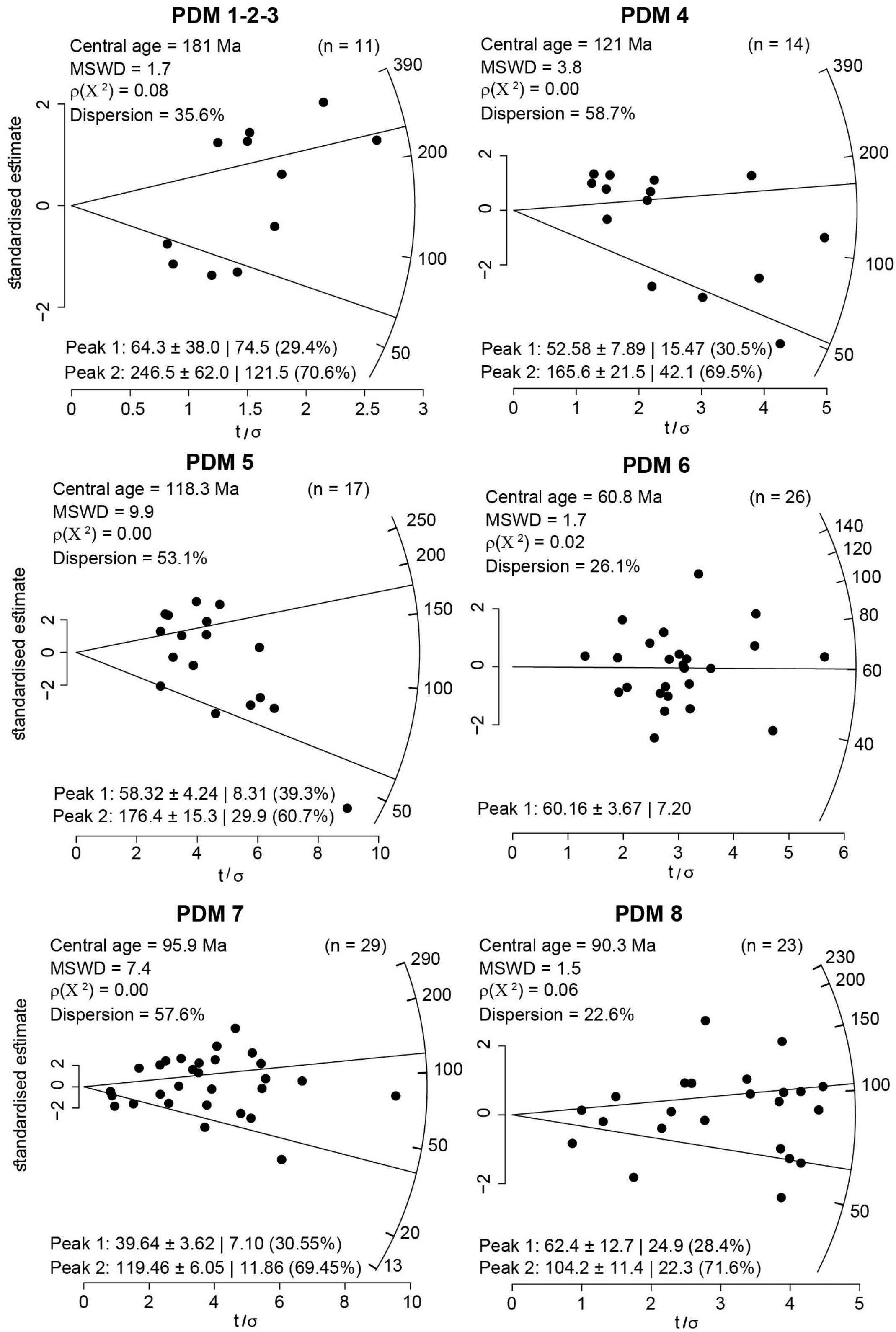

Fig. 9. Radial plots of samples collected in wells from the Rio Grande do Sul with AFT age distributions and age peaks. Most samples have central ages with more than 30% of dispersion, suggesting more than one age population.

determining which data reflect the thickening of the sedimentary pile and little variations in the geotherm, from those severely affected by magmatic heat flux.

8. Thermal implications for burial/exhumation history of the southern Paraná Basin

The temperature variations observed in the southern portion of the Paraná Basin based on the integration of new and previous vitrinite

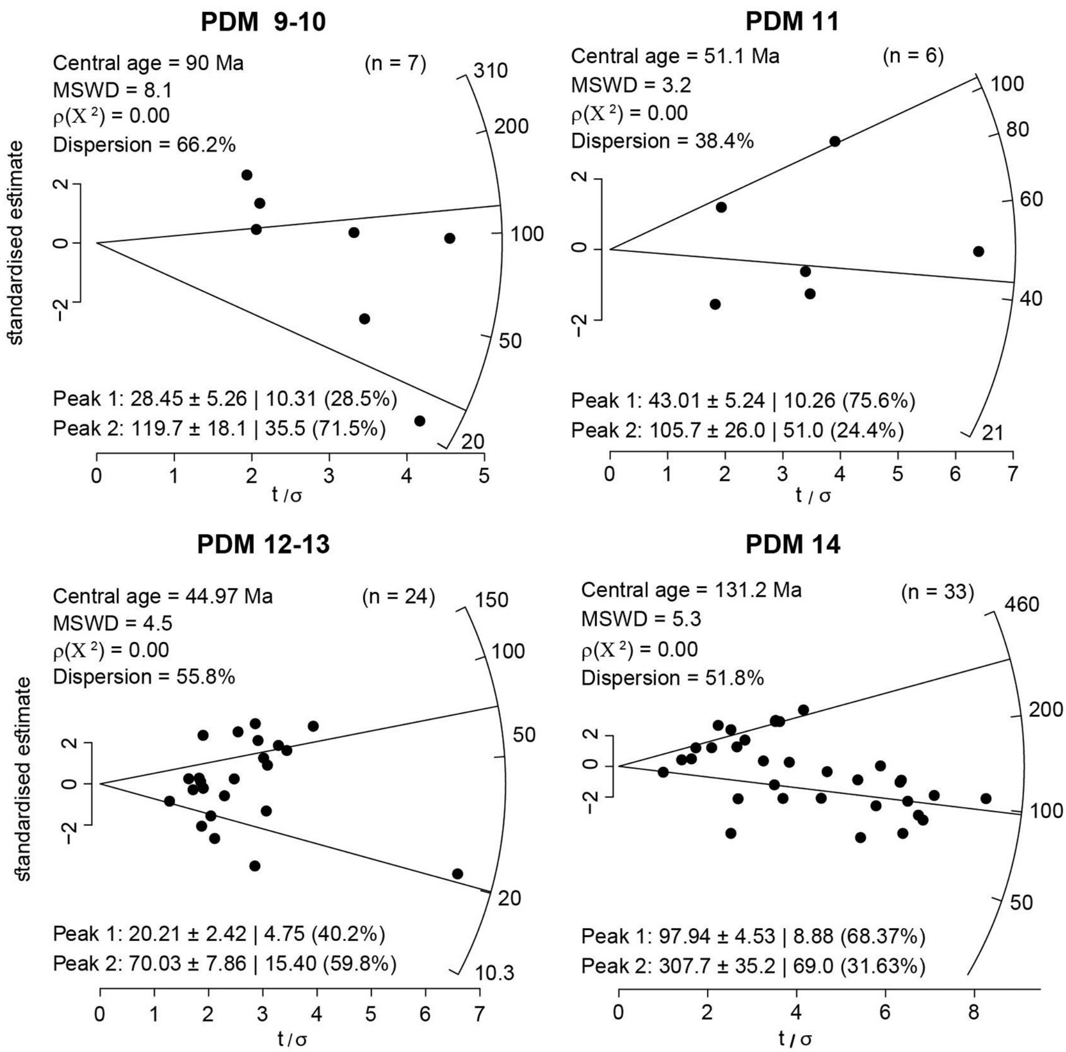

Fig. 10. Radial plots of well samples of southern Santa Catarina with AFT age distributions and age peaks. Most ages are younger than the Serra Geral magmatism, but individual ages have high dispersion.

reflectance and AFT analyses show that the Torres Syncline area had significant importance for the subsidence and magmatism of the basin. Basin temperatures in this region can be attributed to both subsidence and magmatism (secondary geothermal alteration). The distinction between the two is economically relevant. The increase in sedimentary thickness generates higher temperatures and the potential of hydrocarbon generation on a regional scale than temperatures conditioned by local emplacement of igneous intrusions. Four models representing the depositional and erosive history of the basin were constructed based on the observed thermal differences, covering northern Paraná, southern Santa Catarina, and two for the Rio Grande do Sul (Fig. 15A).

8.1. North of Paraná

The sedimentary sequences deposited in northern Paraná (Sapopema area) are thicker if compared to the other studied areas, reaching temperatures close to 50 °C at 250 Ma (Fig. 15B). The Triassic was a period of erosion and/or non-deposition in this part of the basin. The deposition of the Botucatu Formation sandstones, at 150 Ma marks a new episode of subsidence and burial in the basin, which ends with the deposition of 1000 m of lavas from the Serra Geral Formation. The bottom of the sequence reached around 85 °C with a maximum thickness of ca. 2400 m (Fig. 15B). The post-depositional exhumation was established according to the AFT inverse modeling, suggesting that erosion began shortly after the end of deposition in the basin. Vitrinite reflectance values calculated from the burial history range from 0.65 to 0.69%Rr (14B), with an increase of 10 °C depending on the residence time of the coal seams in each temperature interval, that is, higher erosion rates would produce lower reflectances. This temperature corroborates the measured reflectances (0.49–0.74%Rr) and the maximum temperatures determined by the AFT (ca. 80–100 °C) associated with burial history. These data suggest that around 2000–2400 m eroded since Cretaceous in this area (Fig. 15B).

8.2. Sothern Santa Catarina

At the southern Santa Catarina coalfields, the complete sedimentary record of Paraná Basin is also thick (ca. 700 m) and burial history until 150 Ma is similar to the northern Paraná (Fig. 15C). However, in this model, a maximum thickness of 1500 m of igneous rocks was used due to its location at the northeastern edge of the Torres Syncline structure near the Atlantic margin, where magmatism was thicker than inland (Gallagher et al., 1995). The maximum paleotemperature at the basin bottom was around 80–90 °C at 130 Ma (Fig. 15C). The time that had passed since the organic until exhumed to present-day conditions define calculated reflectances of 0.67–0.70%Rr, fitting with the lowest values measured (0.6–0.7%Rr) for that area (Lourenzi and Kalkreuth, 2014; Costa et al., 2014).u The temperature variations recorded by both AFT

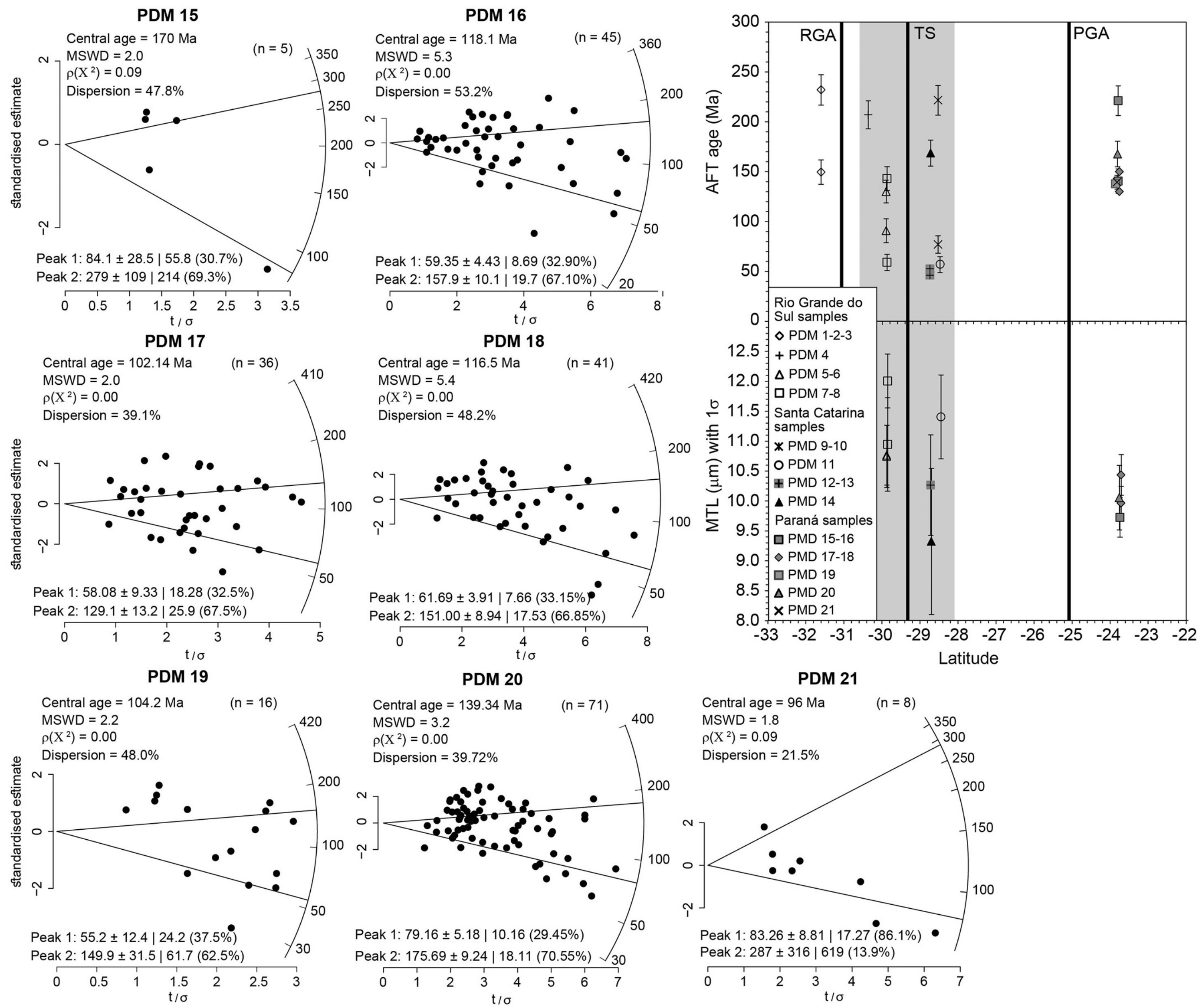

Fig. 11. Radial plots of samples collected in wells from northern Paraná, with AFT age distributions and age peaks, together with a regional evaluation of the AFT ages and MTL of analyzed samples compared with their position to main structural trends. RGA – Rio Grande Arc axis; TS – Torres Syncline axis and area (grey); PGA – Ponta Grossa Arc axis. Most central ages are younger than the Serra Geral magmatism, but individual ages have high dispersion with ages older as Permian.

and vitrinite reflectance data suggest two possible situations to explain such thermal patterns. The first considers the possibility that the thickness of Serra Geral Formation lavas was even higher than the simulated, which would increase the temperature at the basin and higher maturation levels, although the reflectance values higher than 0.8%Rr are commonly associated with the emplacement of igneous intrusions near the coal seams (Kalkreuth et al., 2006, 2010). The second hypothesis assumes an input in temperature during the emplacement of laccoliths within basin sequences affecting surrounding beds, although nor all profiles register igneous rocks interbedded with sediments, implying lateral heating. Assuming the burial history in Fig. 15C, an amount of 1500–2000 m of volcanic and sedimentary material must have been removed from the top of the Paraná sequences, and these amounts are consistent with the estimative of Gallagher et al. (1995).

8.3. Rio Grande do Sul

Southwards, in the models established for the Rio Grande do Sul, the thickness of the sedimentary record is minor than northwards, but increase inland with the addition of the Triassic sediments (Fig. 15D and E). Bottom temperatures do not fit appropriately in the margin model. Still, inland the measured and calculated reflectances and the maximum temperature defined from the AFT inverse modeling are very close to each other, suggesting that the depositional history simulated approaches the reality. However, the burial history of margin samples (Fig. 15D) require a greater thickness of sediments or volcanic rocks to meet the temperatures determined in the region or higher thermal heat flow.

Simulated burial histories reasonably approximate the measured and calculated thermal data, except for samples on the southwest edge of the Torres Syncline (Fig. 15A and D). Raising the volcanic thickness by 500 m would be sufficient enough to increase the calculated reflectance to 0.62%Rr for the same post-depositional history. This supports the hypothesis that the 0.6 to 0.8%Rr reflectance group, commonly found in this area, may have been generated through the burial history of the southern portion of the Paraná Basin, without considering significant variations in the geothermal gradient.

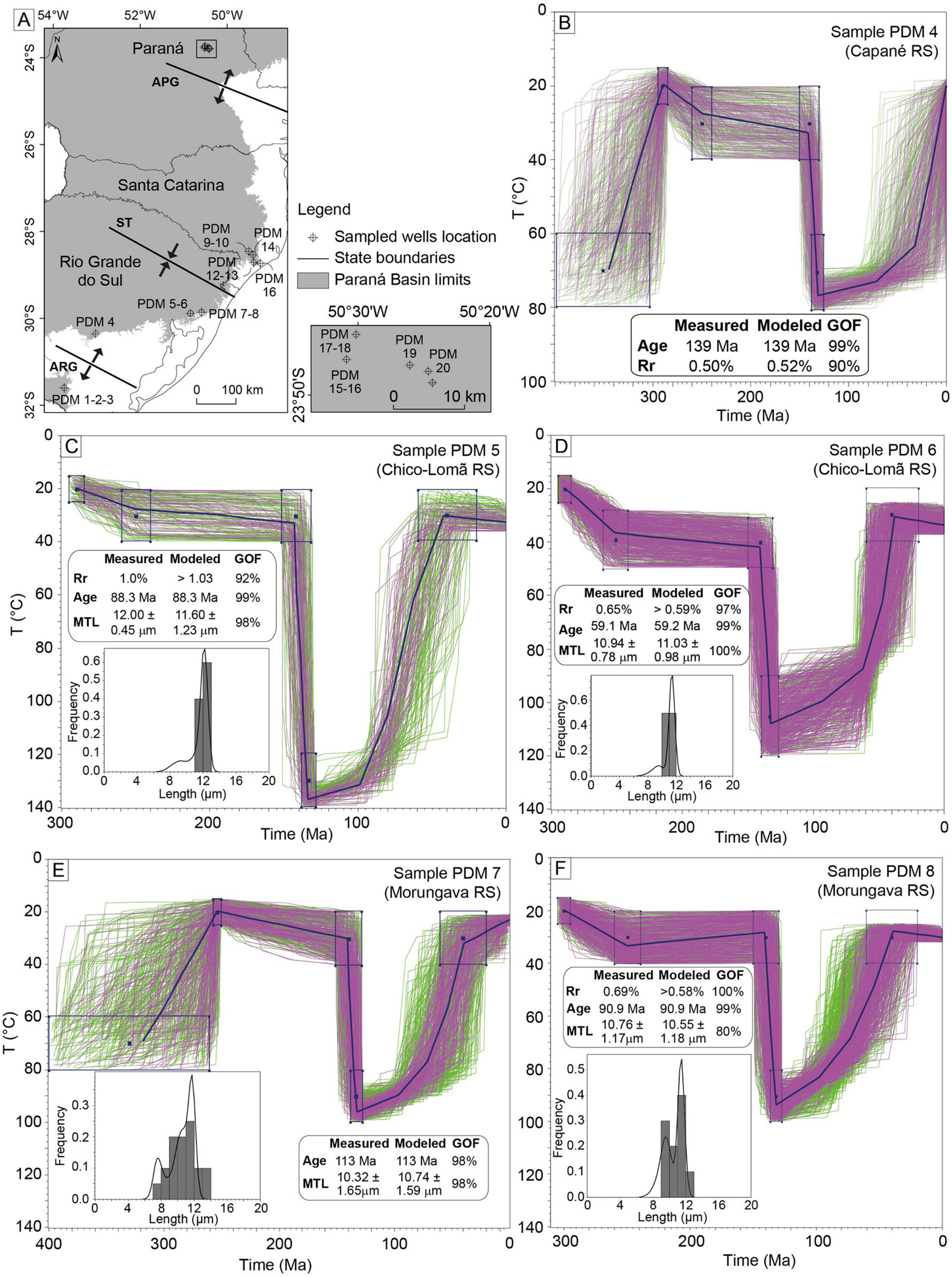

Fig. 12. Location (A) of all samples modeled in this work by AFT technic. Model of Capané (B), Chico-Lomã (C and D), and Morungava (E and F) wells.

8.4. Tectonics and post-depositional evolution

The time periods revealed by the AFT ages and thermal histories defined through inverse modeling covers the early stages of separation between South America and Africa plates. The tectonic pulses that accompanied the depositional stages of the basin during the Permian and Triassic periods did not appear to have significantly affected the basin, at least as regards deposition-related thermal parameters, except where locally there was deposition related to the development of rift basins during the Triassic (Fig. 15A; Zerfass et al., 2005; Milani and de Wit, 2008; Philipp et al., 2018). Most of the protract cooling revealed by the AFT inverse modeling, associated with basin exhumation, start after the maximum temperature was reached at 130–134 Ma. This means that a thick basalt pile also covered the margin of the Paraná Basin and possibly part of basement rocks at the present exposed in the basin, as described by Gallagher et al. (1994, 1995). However, the large presence

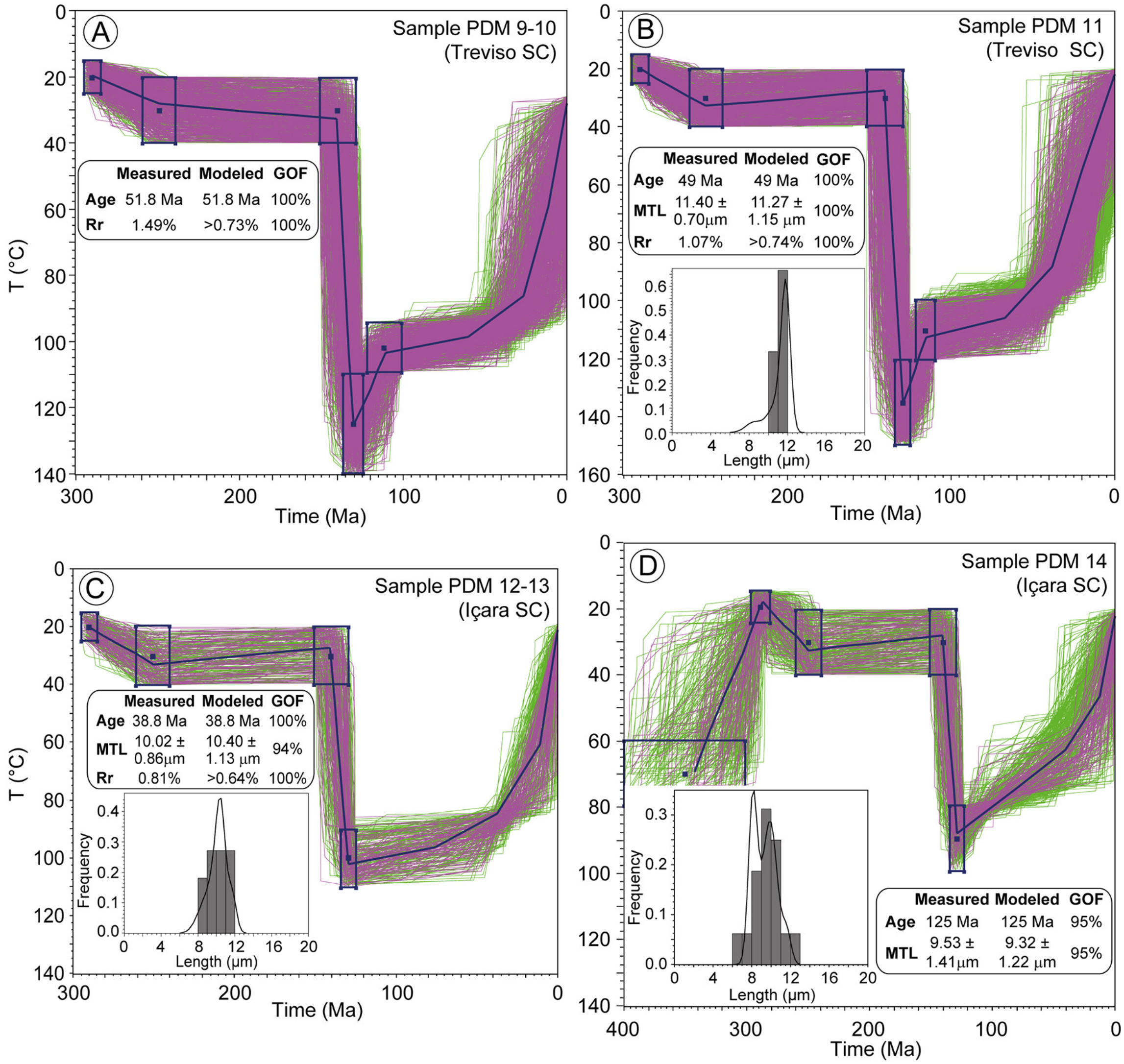

Fig. 13. Apatite thermal modeling of southern Santa Catarina wells. See the map of Fig. 11 for well location. Model of PDM 9–10 (A) and PDM 11 (B) of Treviso location, and PDM 12–13 (C) and PDM 14 (D) of Içara location, southern Santa Catarina.

of individual crystal AFT ages younger than 70 Ma and short MTL measured, reveals an extended period after the Cretaceous magmatism in which some rocks (mostly at the margin of Southern Santa Catarina) experienced a more complex thermal history. This area must have experienced a greater influence of the tectonic and thermal events related to the South Atlantic sea-floor spreading.

The Rio Grande Rise is a volcanic province located in the offshore oceanic lithosphere of the Santos and Pelotas segments of the Brazilian rifted margin, developed during the opening of the South Atlantic Ocean between 90 and 50 Ma (Graça et al., 2019). The opening of the Atlantic has formed structures that extend to the interior of the continental crust, and consequently, the events related to the seafloor spreading may cause subsidence and/or uplift in areas close to these structures. The Ponta Grossa Arc is one of these structures, which has one of the large dikes swarms of Serra Geral magmatism and has a younger thermal history than the Rio Grande Arc (Geraldes et al., 2013; Graça et al., 2019), locally related to hydrothermal processes, but mainly to later erosion related to the uplift of Serra do Mar (Oliveira et al., 2016).

The reactivation of the complex structural framework at the base of the Paraná Basin led to the development of grabens and horsts dividing the basin into several blocks with distinct dimensions. Faulted blocks, mostly at Torres Syncline area, allow the accumulation of thicker sequences, which consequently increase maturity levels of organic beds and favored the preservation of gas deposits adsorbed in coal seams at the coastal region of Rio Grande do Sul (Kalkreuth et al., 2010).

9. Economic potential (oil and gas) of southern Paraná Basin coal, Rio Bonito Formation

Humic coals have little potential for oil generation (Hunt, 1991), although they have an enormous potential for gas generation and storage. The deeply buried coal seams of Rio Grande do Sul and Santa Catarina coasts area 300–1000 m) are, at present, not economical for underground mining. However, the relatively high-rank levels of these coals (Fig. 16A) make them good targets for gas prospection and an alternative source of energy in the southern Paraná Basin. Most of the high-rank coals are located over the Torres Syncline area, where NE-SW and NW-SE structural trends host several igneous intrusions that locally elevates the reflectances value from 0.6–0.8% to > 0.8%Rr in comparison with the other analyzed areas (Fig. 16A). The combination of considerable subsidence, thick sedimentation, and minor post-deposition exhumation kept coal seams for a longer period within the wet-gas generation window (Fig. 16A). Later burial by Cenozoic sediments interrupts the exhumation of Paraná Basin sequences, keeping coals deeply buried and preserving the gas adsorbed into the beds.

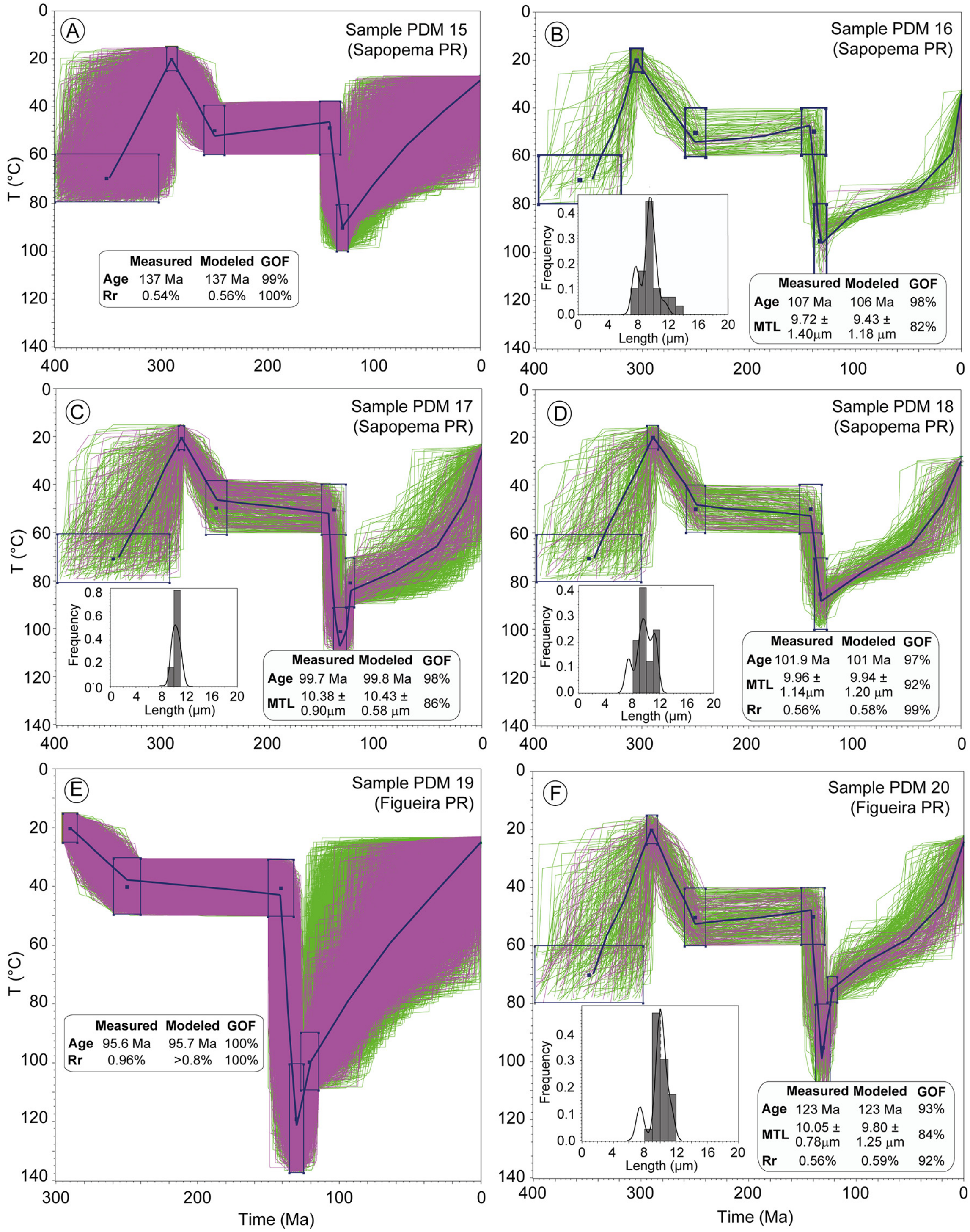

Fig. 14. Apatite thermal modeling of northern Paraná wells. See the map of Fig. 12 for well location. Models of Sapopema coalfield of well WPR 01 (A and B) and WPR 02 (C and D), whereas samples PDM 19 (E) and PDM 20 (F) are from Figueira coalfield.

The high maturity levels identified in the Santa Terezinha and southern Santa Catarina coal layers favor the production of natural gas (Karweil, 1969). However, the methane storage capacity in coal is dependent on several parameters such as mineral and organic matter content, coal type and rank, burial depth, humidity, and rock fabric (Lamberson and Bustin, 1993). Analyses of Santa Terezinha Coalfield gas composition revealed high methane contents (94.26 to 99.47%) of mixed origin (biogenic and thermogenic) indicated by Carbon isotope values from −50.85 to −55.54‰ δ13C. Estimates suggest that there is a total of 5.482 billion m^3 of methane in the Santa Terezinha Coalfield (Kalkreuth et al., 2013a). Coals of the southern Santa Catarina Coalfields also have favorable rank levels for gas production (Fig. 16A); however, all gas produced was lost by widespread natural desorption caused by post-depositional exhumation and loss of confining pressure in the basin required for gas retention within the coal seams (Lourenzi and Kalkreuth, 2014).

9.1. Bituminous Shale of Irati Formation

The Irati Formation contains organic-rich bituminous shales located

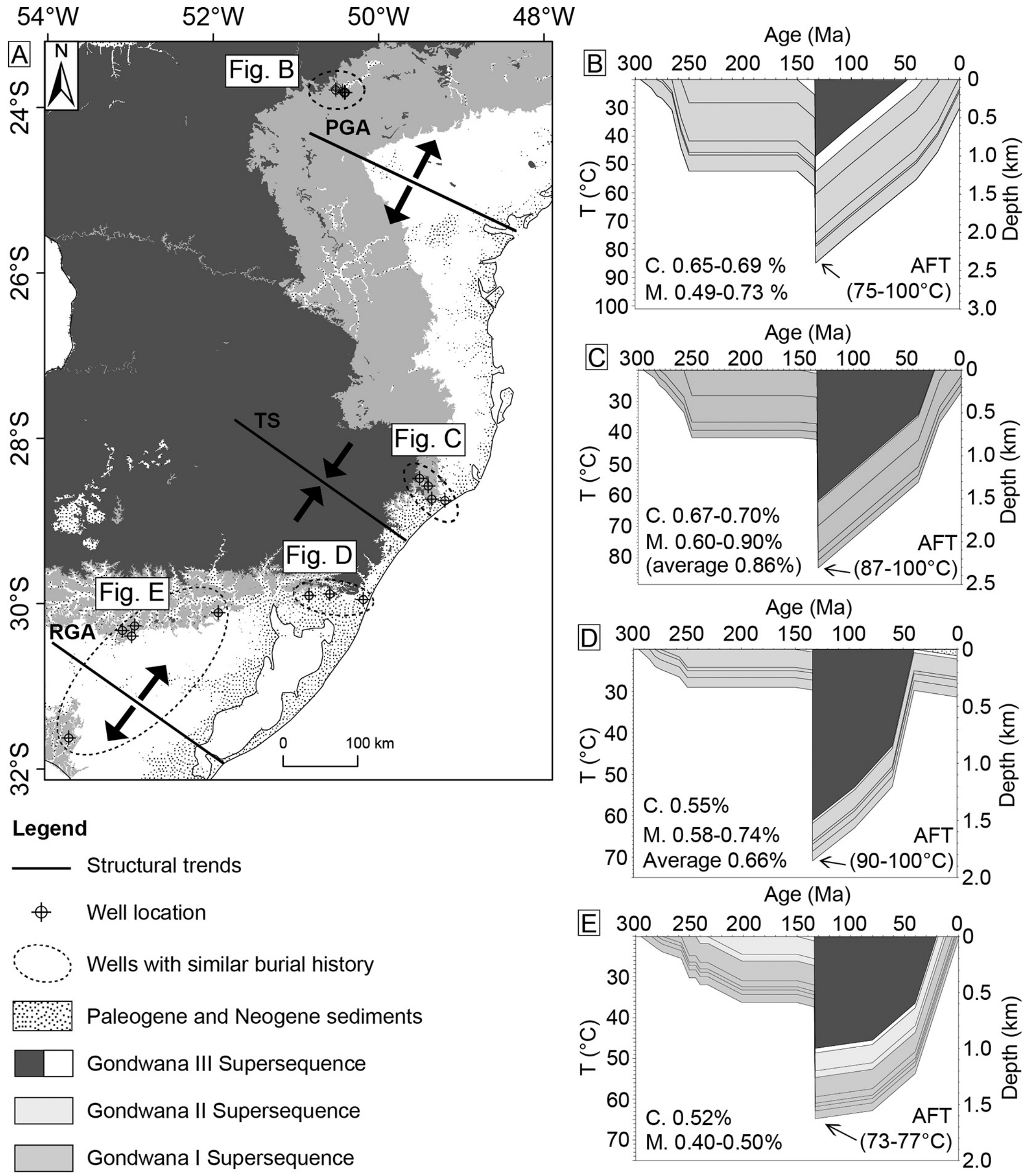

Fig. 15. Geological and structural map of southern Paraná Basin (A) and four probable burial histories, with each calculated (C) and measured (M) vitrinite reflectances. B) Sapopema and Figueira; C) southern Santa Catarina; D and E are for the coast and hinterland of Rio Grande do Sul, respectively. The temperature range measured from thermochronology modeling is also presented for comparison, but only the temperatures attributed to burial are presented. Burial history was based in a constant geotherm (27.5 °C/km) through time, the thickness of strata, vitrinite reflectance, and AFT data. RGA – Rio Grande Arc; TS – Torres Syncline; PGA – Ponta Grossa Arc. Calculations of vitrinite reflectances were based in Waples (1980).

about 100–150 m above the Rio Bonito Formation. Strata of the Irati Formation probably experienced a similar thermal history (Fig. 16B); that is, where coals have reached thermal maturity consistent with the oil/gas generation window, the same can be expected for Irati Formation. This formation has kerogen of Types I and II of amorphous, predominant algal/microbial origin, and Type III, of predominantly terrestrially derived organic matter (Silva and Cornford., 1985; Afonso et al., 1994). Nonetheless, the general immature level found in these beds, as observed from coal seams, limits the potential of Irati Formation as a hydrocarbon source (Silva and Cornford., 1985; Afonso et al., 1994). Apparently, in the Paraná Basin, the Irati Formation had reached a maximum paleoburial of about 1.3–2.8 km (Silva and Cornford, 1985), consistent with the burial history of this work (Fig. 16B).

10. Conclusion

The present study indicates:

1) The rank of coals between 0.4 and 0.6 and 0.6–0.8%Rr are consistent with temperatures of 70–90 and 100 to 110 °C determined by AFT modeling, whereas the intrusion of igneous rocks within the coal seams of Rio Bonito Formation increased temperatures above 135 °C (maximum temperature record by AFT modeling) and reflectances up to 5.0%Rr, with very distinct patterns in comparison to those samples with no influence of the magmatism.
2) The sandstone samples related to lower reflectance patterns (0.4–0.8%Rr) shown partially reset tracks, preserving AFT ages older than the stratigraphic age of the bed. Otherwise, the samples severely heated by the magmatism provide Cretaceous and Early

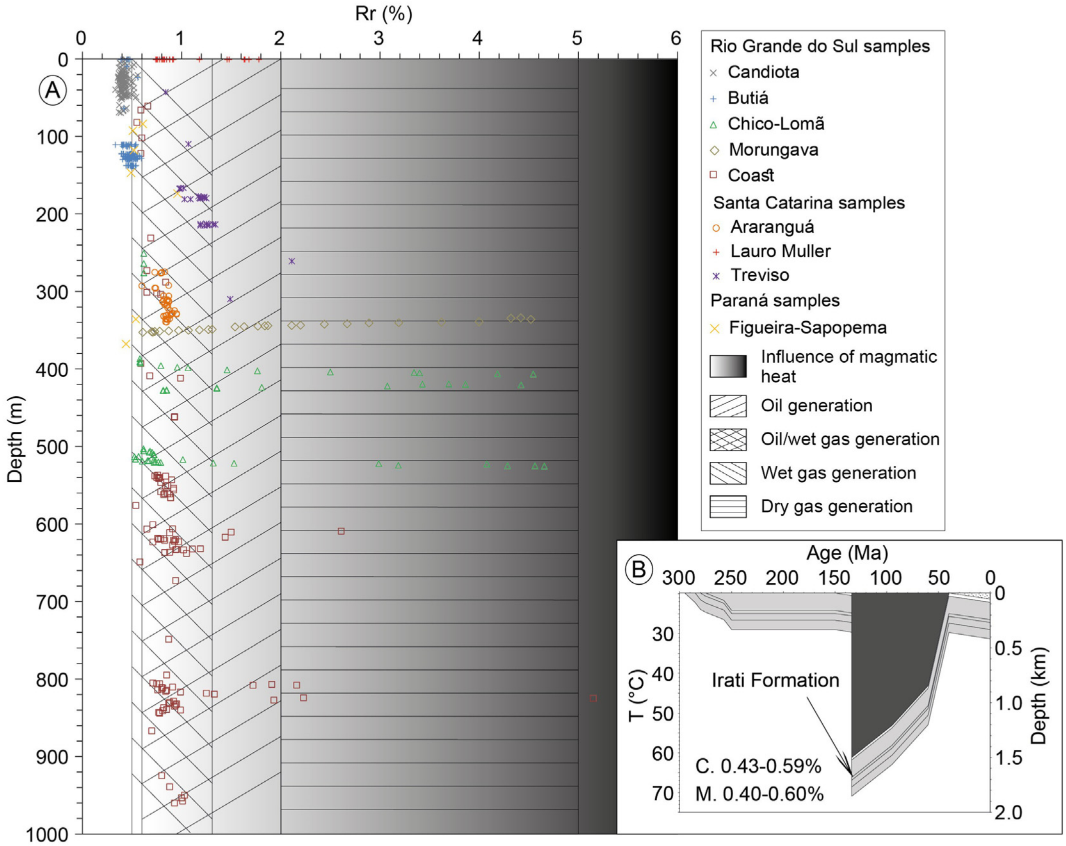

Fig. 16. A) Synthesis of the data and reflectance of vitrinite for the studied areas relating the temperatures/reflectance obtained with the depths of the samples and comparing with the phases of maturation of the organic matter (data of this work; Kalkreuth et al., 2006, 2010, 2013a, 2013b; Silva et al., 2008; Levandowski and Kalkreuth, 2009; Levandowski, 2013; Lourenzi and Kalkreuth, 2014; Costa et al., 2014; Simão and Kalkreuth, 2017). B) Probable burial history of Irati Formation at the Chico-Lomã area with calculated and measured reflectances (Silva and Cornford, 1985).

Cenozoic ages; some are much younger than the last magmatic event, implying deep burial before cooling onset. The MTL distribution of the partially reset samples is short due to the inheritance of tracks preserved from basement cooling history. However, the population of fully reset samples gives crucial information on the maximum temperature reached and the age when cooling onset. At these conditions, around 1.0 to 3.0 km of the Paraná Basin sequences would have been removed from the surface of the studied areas by erosion since Cretaceous and locally from Paleogene. Different amounts of the removed sections were controlled by the structural framework, mostly regional NW-SE and NE-SW oriented structures.

3) The burial history reconstructions suggest that the successive basalt floods over the sedimentary sequences contribute significantly to coalification. In the hinterland of Rio Grande do Sul and Paraná, the simulations with 1.0 km thick of volcanic were sufficient to produce reflectances between 0.5 and 0.7%Rr, consistent with the reflectances measured and with temperatures of AFT modeling. However, at the Torres Syncline area, burial history needs 1.5 km of volcanic rocks to fit with the measured data (0.8%Rr reflectance and AFT temperatures between 100 and 110 °C). This suggests that during magmatism, the geotherm was temporarily higher than the present, with temperatures between 30 and 40 °C; another option is that the thickness of flood basalts at the top was greater than the one used for burial history reconstructions.
4) The intrusion of igneous rocks near coal seams partially improves gas generation and the prospective potential of the southern Paraná Basin. However, basin decompression during periods of exhumation led to gas lost were coal seams were brought to near-surface conditions (mostly in the south of Santa Catarina).

Declaration of Competing Interest

The authors declare that they have no known competing financial interests or personal relationships that could have appeared to influence the work reported in this paper.

Acknowledgments

This study is part of the first author's postdoctoral project developed at the Institute of Geosciences of the Federal University of Rio Grande do Sul. We thank the National Council for Scientific and Technological Development (CNPq) of Brazil for financial support for the junior postdoctoral fellowship (150550_2017-0) of the first author and to a CNPq Research Grant for W. Kalkreuth. We also thank the Carbonífera do Cambuí, Copelmi and Rio Deserto mining companies for the availability of sample collection and logistical support.

References

Afonso, J.C., Schmal, M., Cardoso, J.N., 1994. Hydrocarbon distribution in the lrati shale oil. Fuel 73 (3), 363–366.
Araújo, L.M., Trigüis, J.A., Cerqueira, J.R., Freitas, L.C. da S., 2000. The Atypical Permian Petroleum System of the Paraná Basin, Brazil. In: Mello M.R., Katz B.J. (Eds.), Petroleum Systems of South Atlantic Margins. AAPG Mem. 73, 377–402.
Araújo, C.C., Yamamoto, J.K., Rostirolla, S.P., Madruccia, V., Tankard, A., 2005. Tar sandstones in the Paraná Basin of Brazil: structural and magmatic controls of hydrocarbon charge. Mar. Petrol. Geol. 22, 671–685.
Bustin, R., Cameron, A., Grieve, D., Kalkreuth, W.D., 1989. Coal Petrology — Its Principles, Methods and Applications, Geol. Assoc. Canada, Short Course Notes, V.3, Victoria, British Columbia, Third Edition. pp. 273.
Cagliari, J., Lavina, E.L.C., Philipp, R.P., Tognoli, F.M.W., Basei, M.A.S., Faccini, U.F., 2014. New Sakmarian ages for the Rio Bonito formation (Paraná Basin. Southern Brazil) based on LA-ICP-MS U-Pb radiometric dating of zircons crystals. J. S. Am.

Earth Sci. 56, 265–277.
Cagliari, J., Philipp, R.P., Buso, V.V., Netto, R.G., Hillebrand, P.K., da Cunha Lopes, R., Basei, M.A.S., Faccini, U.F., 2016. Age constraints of the glaciation in the Paraná Basin: evidence from new U-Pb dates. J. Geol. Soc. 173 (6), 871–875.
Canile, F.M., Babinski, M., Rocha-Campos, A.C., 2016. Evolution of the Carboniferous-Early Cretaceous units of Paraná Basin from provenance studies based on U-Pb, Hf and O isotopes from detrital zircons. Gondwana Res. 40, 142–169.
Choate, R., McCord, J., Rightmire, C., 1986. Assessment of natural gas from coalbeds by geologic characterization and production evaluation. In: Rice, D. (Ed.), Oil and Gas Assessment. AAPG Studies Geol. 21, 223–245.
Costa, J.B., Lourenzi, P.S., González, M.B., Peralba, M.C.R., Kalkreuth, W., 2014. A petrological and organic geochemical study of Permian coal seams east of Maracajá, South Santa Catarina, Paraná Basin, Brazil. Int. J. Coal Geol. 132, 51–59.
Donelick, R.A., O'Sullivan, P.B., Ketcham, R.A., 2005. Apatite fission-track analysis. In: Reiners, P.W., Ehlers, T.A. (Eds.), Low-Temperature Thermochronology: Techniques, Interpretations, and Applications. vol. 58. Mineral. Soci. Am, Washington, pp. 49–94 Reviews in Mineralogy and Geochemistry.
Duddy, I.R., Green, P.F., Hegarty, K.A., Bray, R.J., O'Brien, G.W., 1998. Dating and duration of hot fluid flow events determined using AFTA® and vitrinite reflectance-based thermal history reconstruction. In: Parnell, J. (Ed.), Dating and duration of hot fluid flow and fluid-rock interaction. 144. pp. 41–51 Geol. Soci. Speci. Publ. (London).
Galbraith, R.F., Laslett, G.M., 1993. Statistical models for mixed fission track ages. Nucl. Tracks Radiat. Meas. 21, 459–470.
Gallagher, K., 2012. Transdimensional inverse thermal history modeling for quantitative thermochronology. J. Geophys. Res. 117.
Gallagher, K., Hawkesworth, C.J., Mantovani, M.S.M., 1994. The denudation history of the onshore continental margin of SE Brazil inferred from apatite fission track data. J. Geophys. Res. 99 (B9), 18117–18145.
Gallagher, K., Hawkesworth, C.J., Mantovani, M.S.M., 1995. Denudation, fission track analysis and the long-term evolution of passive margin topography: application to the southeast Brazilian margin. J. S. Am. Earth Sci. 8, 65–77.
Gallagher, K., Brown, R., Johnson, C., 1998. Fission track analysis and its applications to geological problems. Annu. Rev. Earth Planet. Sci. 26, 519–572.
Geraldes, M.C., Motoki, A., Costa, A., Mota, C.E., Mohriak, W.E., 2013. Geochronology (Ar/Ar and K–Ar) of the South Atlantic post-break-up magmatism. Geol. Soc. London, Spec. Publ. 369, 41–74.
Gleadow, A.J.W., 1981. Fission track dating methods: what are the real alternatives? Nucl. Tracks Radiat. Meas. 5, 3–14.
Gleadow, A.J.W., Belton, D.X., Kohn, B.P., Brown, R.W., 2002. Fission track dating of phosphate minerals and the thermochronology of apatite. In: Kohn, M.J., Rakovan, J., Hughes, J.M. (Eds.), Phosphates, Geochemical, Geobiological, and Materials Importance, Reviews in Mineralogy and Geochemistry. vol. 48. Mineral. Soci. Am, Washington, D.C, pp. 579–630.
Goodarzi, F., Gentzis, T., Dewing, K., 2019. Influence of igneous intrusions on the thermal maturity of organic matter in the Sverdrup Basin, Arctic Canada. Int. J. Coal Geol. 213, 103280. https://doi.org/10.1016/j.coal.2019.103280.
Graça, M.C., Kusznir, N., Stanton, N.S.G., 2019. Crustal thickness mapping of the central South Atlantic and the geodynamic development of the Rio Grande Rise and Walvis Ridge. Mar. Petrol. Geol. 101, 230–242.
Green, P.F., Duddy, I.R., Gleadow, A.J.W., Tingate, P.R., Laslett, G.M., 1986. Thermal annealing of fission tracks in apatite 1. A Qualitative Description. Chem. Geol. 59, 237–253.
Green, P.F., Duddy, I.R., Laslett, G.M., Hegarty, K.A., Gleadow, A.J.W., Lovering, J.F., 1989. Thermal annealing of fission tracks in apatite 4. Quantitative modelling techniques and extension to geological timescales. Chem. Geol. 79, 155–182.
Green, P.F., Crowhurst, P.V., Duddy, I.R., 2004. Integration of AFTA and (U-Th)/He thermochronology to enhance the resolution and precision of thermal history reconstruction in the Anglesea-1 well. Otway Basin, SE Australia. In: PESA Eastern Australasian Basins Symposium II, Adelaide, pp. 19–22.
Griffis, N.P., Mundil, R., Montañez, I.P., Isbell, J., Fedorchuk, N., Vesely, F., Iannuzzi, R., Yin, Q.Z., 2018. A new stratigraphic framework built on U-Pb single-zircon TIMS ages and implications for the timing of the penultimate icehouse (Paraná Basin, Brazil). Geol. Soc. Am. Bull. 130, 848–858. https://doi.org/10.1130/B31775.1.
Guerra-Sommer, M., Cazzulo-Klepzig, M., Menegat, R., Formoso, M.L.L., Basei, M.A.S., Barboza, E.G., Simas, M.W., 2008a. Geochronological data from the Faxinal coal sucession, Southern Paraná Basin, Brazil: a preliminar approach combining radiometric U-Pb dating and palynostratigraphy. J. S. Am. Earth Sci. 25, 246–256.
Guerra-Sommer, M., Cazzulo-Klepzig, M., Formoso, M.L.L., Menegat, R., Fo, J.G.M., 2008b. U-Pb dating of tonstein layers from a coal succession of the Southern Paraná Basin (Brazil): a new geochronological approach. Gondwana Res. 14, 474–482.
Guerra-Sommer, M., Cazzulo-Klepzig, M., Santos, J.O.S., Hartmann, L.A., Ketzer, J.M., Formoso, M.L.L., 2008c. Radiometric age determination of tonsteins and stratigraphic constrains for the Lower Permian coal succession in Southern Paraná Basin. Brazil. Int. J. Coal Geol. 74, 13–27.
Guo, P.Y., Zhang, N., He, M.C., Bai, B.H., 2017. Effect of water saturation and temperature in the range of 193 to 373 K on the thermal conductivity of sandstone. Tectonophysics 699, 121–128.
Hamza, V.M., Dias, F.J.S.S., Gomes, A.J.L., Terceros, Z.G.D., 2005. Numerical and functional representations of regional heat flow in South America. Phys. Earth Planet. Inter. 152, 223–256.
Hartmann, L.A., Baggio, S.B., Brückmann, M.P., Knijnik, D.B., Lana, C., Massonne, H.J., Opitz, J., Pinto, V.M., Sato, K., Tassinari, C.C.G., Arena, K.R., 2019. U-Pb geochronology of Paraná volcanics combined with trace element geochemistry of the zircon crystals and zircon Hf isotope data. J. S. Am. Earth Sci. 89, 219–226.
Holz, M., Kalkreuth, W., 2004. Sequence Stratigraphy and Coal Petrology applied to the Early Permian coal-bearing Rio Bonito Formation, Paraná Basin, Brazil. In: Pashin, J., Gastaldo, R. (Eds.), Sequence Stratigraphy, Paleoclimate, and Tectonics of Coal-Bearing Strata. AAPG Studies Geol. 51, 147–167.
Holz, M., Kalkreuth, W., Banerjee, I., 2002. Sequence stratigraphy of coal-bearing strata: an overview. Int. J. Coal Geol. 48, 147–179.
Holz, M., Küchle, J., Philipp, R.P., Bischoff, A.P., Arima, N., 2006. Hierarcy of tectonic control on stratigraphic signatures: Base-level changes during the Early Permian in the Paraná Basin, southernmost Brazil. J. S. Am. Earth Sci. 22, 185–204.
Holz, M., França, A.B., Souza, P.A., Iannuzzi, R., Rohn, R., 2010. A stratigraphic chart of the Late Carboniferous/Permian succession of the eastern border of the Paraná Basin, Brazil, South America. J. S. Am. Earth Sci. 29, 381–399.
Hunt, J.M., 1991. Generation of gas and oil from coal and other terrestrial organic matter. Org. Geochem. 17, 673–680.
Hurford, A.J., 1990. International union of geological sciences subcommission on geochronology recommendation for the standardization of fission track dating calibration and data reporting. Nucl. Tracks Radiat. Meas. 17 (3), 233–236.
ISO-7404/5, 2009. Methods for the petrographic analysis of coals. Part 5: Method of determining Microscopically the Reflectance of Vitrinite. Int. Org. for Standar (14p).
Kalkreuth, W., McMechan, M., 1984. Regional pattern of thermal maturation as determined from coal-rank studies, Rocky Mountain Foothills and Front Ranges north of Grande Cache, Alberta – Implications for petroleum generation. Bull. Can. Petrol. Geol. 249–271.
Kalkreuth, W., Langenberg, W., McMechan, M., 1989. Regional coalification pattern of Lower Cretaceous coal-bearing strata, Rocky Mountain Foothills and foreland, Canada - implications for future exploration. Int. J. Coal Geol. 13, 261–302.
Kalkreuth, W., Holz, M., Kern, M., Machado, G., Mexias, A., Silva, M.B., Willett, J., Finkelman, R., Burger, H., 2006. Petrology and chemistry of Permian coals from the Paraná Basin: 1. Santa Terezinha. Leão-Butiá and Candiota Coalfields, Rio Grande do Sul. Brazil. Int. J. Coal Geol. 68, 79–116.
Kalkreuth, W., Holz, M., Mexias, A., Balbinot, M., Levandowski, J., Willett, J., Finkelman, R., Burger, H., 2010. Depositional setting. Petrology and chemistry of Permian coals from the Paraná Basin: 2. South Santa Catarina Coalfield. Brazil. Int. J. Coal Geol. 84, 213–236.
Kalkreuth, W., Holz, M., Levandowski, J., Kern, M., Casagrande, J., Weniger, P., Krooss, B., 2013a. The coalbed methane (CBM) potential and CO2 storage capacity of the Santa Terezinha Coalfield. Paraná Basin. Brazil – 3D modelling and coal and carbonaceous shale characteristics and related desorption and adsorption capacities in samples from exploration Borehole CBM001-ST-RS. Energy Explor. Exploit. 31 (4), 485–527.
Kalkreuth, W., Lunkes, M., Oliveira, J., Ghiggi, M.L., Osório, E., Souza, K., Sampaio, C.H., Hidalgo, G., 2013b. The lower and upper coal seams of the Candiota Coalfield. Brazil - Geological setting, petrological and chemical characterization, and studies on reactivity and beneficiation related to their combustion potential. Int. J. Coal Geol. 111, 53–66.
Karweil, J., 1969. Actuelle Probleme der Geochemie der kohle. In: Advances in Org. Geochem. Oxford. Pergamon Press, pp. 59–84.
Ketcham, R.A., 2005. Forward and inverse modeling of low temperature thermochronometry data. In: Reiners, P.W., Ehlers, TA. (Eds.), Low-Temperature Thermochronology. Rev. Mineral. Geochem. 58, 275–314.
Ketcham, R.A., Carter, A.C., Donelick, R.A., Barbarand, J., Hurford, A.J., 2007. Improved modeling of fission-track annealing in apatite. Am. Mineral. 92, 799–810.
Lamberson, M.N., Bustin, R.M., 1993. Coalbed methane characteristics of Gates Formation Coals, Northeastern British Columbia: effect of Maceral Composition. AAPG Bull. 77 (12), 2062–2076.
Laslett, G.M., Green, P.F., Duddy, I.R., Gleadow, A.J.W., 1987. Thermal annealing of fission tracks in apatite 2. A quantitative analysis. Chem. Geol. 65, 1–13.
Levandowski, J.H., 2013. Características Petrográficas e Geoquímicas das Camadas de Carvão Do Poço CBM 001 – CL – RS. Bacia Do Paraná. Petrographical and Geochemical Characteristics of Coal Seams Collected from Borehole CBM 001 – CL – RS. Ph.D thesis, text in Portuguese with English abstract. Universidade Federal do Rio Grande do Sul. Instituto de Geociências, Porto Alegre, pp. 92.
Levandowski, J., Kalkreuth, W., 2009. Chemical and petrographical characterization of feed coal. Fly ash and bottom ash from the Figueira Power Plant, Paraná, Brazil. Int. J. Coal Geol. 77, 269–281.
Lopatin, N., 1971. Temperature and geologic time as factors in coalfication. Acad. Nauk SSSR Ivz. Ser. Geol. 3, 95–106.
Lopes, R.C., Peruffo, N., Sachs, L.L.B., Silva, V.A., Batista, I.H., 2004. Folha Paranapanema SF 22. In: Schobbenhaus, C., Gonçalves, J.H., Santos, J.O.S. (Eds.), Carta Geológica do Brasil ao Milionésimo, Sistema de Informações Geográficas. Programa Geologia do Brasil. Geologica Map of Brazil, Geographical Information System, Brazilian Geological Program, CPRM- Geological Survey of Brazil, Brasília CD-ROM.
Lourenzi, P.D., Kalkreuth, W., 2014. O potencial de geração CBM (Coalbed Methane) na jazida Sul Catarinense: 1. Características petrográficas e químicas das camadas de carvão da Formação Rio Bonito, Permiano da Bacia do Paraná. The CBM (Coalbed Methane) generation potential in the Sul Catarinense coalfield: 1. Petrographical and chemical characteristics of coals from the Permian Rio Bonito Formation, Paraná Basin, text in Portuguese with English abstract. Braz. J. Geol. 44 (3), 471–491.
Milani, E.J., de Wit, M.J., 2008. Correlations between the classic Paraná and Cape–Karoo sequences of South America and southern Africa and their basin infills flanking the Gondwanides: du Toit revisited. In: Pankhurst, R.J., Trouw, R.A.J., Brito Neves, B.B., De Wit, M.J. (Eds.), West Gondwana: Pre-Cenozoic Correlations Across the South Atlantic Region, pp. 319–342 Geol. Soci. London. Spec. Public. 294.
Mori, A.L.O., Souza, P.A., Marques, J.C., Lopes, R.C., 2012. A new U-Pb zircon age dating and palynological data from a Lower Permian section of the southernmost Paraná Basin, Brazil: biochronostratigraphical and geochronological implications for

Gondwanan correlations. Gondwana Res. 21, 654–669.
Oliveira, C.H.E., Jelinek, A.R., Chemale, F., Cupertino, J.A., 2016. Thermotectonic history of the southeastern Brazilian margin: evidence from apatite fission track data of the offshore Santos Basin and continental basement. Tectonophysics 685, 21–34.
Perrotta, M.M., Salvador, E.D., Lopes, R.C., D'Agostino, L.Z., Wildner, W., Ramgrab, G.E., Peruffo, N., Freitas, M.A., Gomes, S.D., Chieregati, L.A., Silva, L.C., Sachs, L.L.B., Silva, V.A., Batista, I.H., Marcondes, P.E.P., 2004. Folha Curitiba SG-22. In: Schobbenhaus, C., Gonçalves, J.H., Santos, J.O.S. (Eds.), Carta Geológica do Brasil ao Milionésimo, Sistema de Informações Geográficas. Programa Geologia do Brasil. Geological map of Brazil, Geographical Information System, Brazilian Geological Program, CPRM- Geological Survey of Brazil, Brasília CD-ROM.
Philipp, R.P., Schultz, C.L., Kloss, H.P., Horn, B.L.D., Soares, M.B., Basei, M.A.S., 2018. Middle Triassic SW Gondwana paleogeography and sedimentary dispersal revealed by integration of stratigraphy and U-Pb zircon analysis: the Santa Cruz Sequence, Paraná Basin, Brazil. J. S. Am. Earth Sci. 88, 216–237.
Saghafi, A., Pinetown, K.L., Grobler, P.G., van Heerden, J.H.P., 2008. CO2 storage potential of South African coals and gas entrapment enhancement due to igneous intrusions. Int. J. Coal Geol. 73, 74–87.
Santos, R.V., Souza, P.A., Alvarenga, C.J.S., Dantas, E.L., Pimentel, M.M., Oliveira, C.G., Araújo, L.M., 2006. SHRIMP U-Pb zircon dating and palynology of bentonitic layers from the Permian Irati Formation, Paraná Basin, Brazil. Gondwana Res. 9, 456–463.
Silva, Z.C.C., Cornford, C., 1985. The kerogen type, depositional environment and maturity, of the lrati Shale, Upper Permian of Paraná Basin, Southern Brazil. Org. Geochem. 8 (6), 399–411.
Silva, M.B., Kalkreuth, W., Holz, M., 2008. Coal petrology of coal seams from the Leão-Butiá Coalfield, Lower Permian of the Paraná Basin, Brazil — Implications for coal facies interpretations. Int. J. Coal Geol. 73, 331–358.
Simão, G., Kalkreuth, W., 2017. O carvão da Jazida de Morungava (RS, Brasil): Caracterização petrográfica, química e tecnológica das camadas de carvão do poço de exploração CBM 001-MO-RS. The coal in the Morungava Coalfield (RS, Brazil): Petrographical, chemical and technological characteristics of coals collected from exploration borehole CBM 001-MO-RS, text in Portuguese with English abstract. Pest Geosci 44 (2), 323–343.
Simas, M.W., Guerra-Sommer, M., Cazzulo-Klepzing, M., Menegat, R., Santos, J.O.S., Ferreira, J.A.F., Degani-Schmidt, I., 2012. Geochronological correlation of the main coal interval in Brazilian Lower Permian: radiometric dating of tonstein and calibration of biostratigraphic framework. J. S. Am. Earth Sci. 39, 1–15.
Ting, F.T.C., 1978. Petrographic techniques in coal analysis. In: Karr, C.Jr (Ed.), Analytical Methods for Coal and Coal Products. Academic Press. vol. 1. pp. 3–26.
Vermeesch, P., 2018. IsoplotR: a free and open toolbox for geochronology. Geosci. Front. 9, 1479–1493. https://doi.org/10.1016/j.gsf.2018.04.001.
Wagner, G.A., Van den Haute, P., 1992. Fission-Track Dating. Ferdinand Enke Verlag, Stuttgart, pp. 285.
Waples, D., 1980. Time and temperature in petroleum formation: Application of Lopatin's method to petroleum exploration. AAPG Bull. 64, 916–926.
Wildner, W., Ramgrab, G.E., Lopes, R.C., Iglesias, C.M.F., 2008. Mapa Geológico do Estado do Rio Grande do Sul, escala 1:750,000, Geological Map of the state of Rio Grande do Sul, scale 1:750,000. CPRM -Geological Survey of Brazil, Porto Alegre.
Zerfass, H., Chemale Jr., F., Lavina, E.L., 2005. Tectonic control of the Triassic Santa Maria units of the Paraná basin, southernmost Brazil, and its correlation to the Waterberg basin, Namibia. Gondwana Res. 8 (2), 163–176.
Zerfass, H., Chemale Jr., F., Schultz, C.L., Lavina, E.L., 2004. Tectonics and sedimentation in southern South America during Triassic. Sediment. Geol. 166, 265–292.